North Pacific Research Board Project Final Report

Using hair cortisol to assess physiological stress in Alaska polar bears

Project numbers 1716A and 1716B

George M. Durner

U.S. Geological Survey, Alaska Science Center

4210 University Drive

Anchorage, Alaska 99508 USA

907-786-7082

gdurner@usgs.gov

October 2020

Contents

Abstract

The concentration of cortisol in hair (HCC) of polar bears (*Ursus maritimus*) may provide a retrospective view of physiological stress they experience and a link to their response to environmental change. To understand this relationship, we assayed HCC from polar bears captured in the Alaska Beaufort, Bering and Chukchi seas during 1983–1989 and 2004–2016. Cortisol accumulated in hair through summer and autumn and into the subsequent winter. HCC was similar between adult males and adult females. No difference in HCC across regions suggested all bears responded similarly to the environment. HCC in spring was elevated following years with a high winter Arctic Oscillation index and highly variable wind speed. HCC increased non-linearly with increasing duration of the continental shelf summer open water period up to 50 days and then decreased. HCC of spring samples declined with increasing body size, indicating that the stress response was more active in smaller bears or those in poor body condition. HCC of spring samples was greater and more variable in 2004–2006 than during either 1983–1989 or 2008–2016, and significantly so for females with 1st year cubs and subadult females. Elevated HCC in 2004–2006 coincided with years of reduced survival of southern Beaufort Sea polar bears and suggests that unidentified environmental perturbations impacted Alaska polar bears. Because HCC may be obtained by relatively non-invasive means, it has potential use for assessing polar bear populations that are difficult to study by capturing. Hence, information gained from HCC can inform polar bear conservation, especially on the vulnerability of subadult females and adult females with new cubs, and possible future environmental perturbations impacts on bear physiology.

Key words: Alaska, Beaufort Sea, Bering Sea, Chukchi Sea, cortisol, hair, polar bear, stress response, *Ursus maritimus*

Suggested citation

George M. Durner. 2020. Using hair cortisol to assess physiological stress in Alaska polar bears. NPRB Projects 1716A and 1716B Final Report. 79pp.

Introduction

An animal's life is sometimes punctuated by a need to allocate resources for coping with stressors that may negatively impact its survival. The stressor may be predictable, for example circadian or seasonal changes in prey or forage, initiation of migration, competition for mates, or acquisition of resources necessary for breeding. In contrast, acute stressors are usually unpredictable and intense, for example the vigorous pursuit of prey by a predator or equally vigorous escape of the prey. In most situations following an acute stressor, the stress response is relatively brief, and the animal's physiological state returns to a baseline level within hours. The functional role of the stress response is to heighten functions such as blood circulation, breathing and mental acuity, and reallocate energy resources and immune functions, such that survival is maximized. These functions come at the expense of other life history processes including feeding, reproduction and growth.

The general stress response has been reviewed in several publications (e.g., Boonstra 2004, Sapolsky et al. 2000, Smith and Vale 2006). In brief, the stress response consists primarily of two parts with the first initiated by the sympathetic nervous system (hippocampus) and adrenal medulla and the second part with a sequential cascade of events by the hypothalamus, pituitary gland, and the adrenal cortex (i.e., the HPA axis). Within the first several seconds of exposure to a stressor, the sympathetic nervous system signals the adrenal medulla to release catecholamines (epinephrine and norepinephrine) into the blood stream. This process invokes the "flight or fight" response by the animal, as the release of catecholamines increases heart rate, constricts blood vessels in peripheral tissues so more blood is available to skeletal muscles, and increases breathing rate. Energy substrates become more available to the animal through fat catabolism and glucose levels increase through breakdown of glycogen in muscles, increased

glucagon production and reduced production of insulin. The animal's alertness is heightened, and memory is enhanced.

The second part of the stress response involves the production and release of glucocorticoids above baseline levels and is initiated several minutes after a stressor is initially perceived. The role of a glucocorticoid surge largely compliments the function of catecholamines to increase and maintain glucose in the blood. A cascade of events leads to release of glucocorticoids. Neural activity causes the paraventricular nucleus of the hypothalamus to rapidly increase secretion of corticotropin-releasing hormone (CRH) into circulation. The increase in CRH causes the anterior pituitary to secrete adrenocorticotropic hormone (ACTH). The abrupt increase of ACTH in circulation acts upon the adrenal cortex to produce the glucocorticoids corticosterone and/or cortisol. The surge of glucocorticoids boosts energy available to the animal through catabolism of muscle and bone into amino acids that the liver converts to glucose (gluconeogenesis), suppression of insulin, and catabolism of fats into fatty acids as an energy substrate for all tissues except for the brain. Glucocorticoids also reduce inflammation and in doing so reduce tissue damage by the immune system. Because energy mobilization during exposure to an acute stressor is paramount, glucocorticoids suppress reproductive and growth functions by inhibiting the gonadotropin and growth hormones from the anterior pituitary.

Variation in the level of glucocorticoids to cope with seasonality of environmental conditions and life history, such as prey or forage availability and reproduction, and responding to short term stressors like chasing prey or escape from a predator, is an adaptive trait that maintains fitness. However, prolonged elevated glucocorticoids resulting from chronic stress may be deleterious, especially when coupled with periodic acute stress. Physiological impacts of

elevated glucocorticoids over long periods may include hypertension (Whitworth et al. 2005), muscle atrophy (Braun and Marks 2015) and bone wasting (Turnlund et al. 1979), down regulation of immune functions (Morey et al. 2015), reproductive suppression (Kirby et al. 2009, Tilbrook et al. 2000), and negative impacts to cognitive function and memory retrieval (de Quervain et al. 1998). Perhaps counterintuitively, chronic stress may serve to suppress both baseline glucocorticoid levels and glucocorticoid response to severe stress (Rich and Romero 2005). Environmental events that lead to atypical glucocorticoid levels in wildlife may include long-term fasting (Barcellos et al. 2010, Nakamura et al. 2016, Ortiz et al. 2001), habitat degradation (Narayan 2019), contaminant exposure (Hontela et al. 1992), human-induced trauma (Gentsch et al. 2018), and social interactions (i.e., crowding; Pearson et al. 2015).

Assessment of glucocorticoids derived from tissue samples may elucidate a link between the response of wildlife health and their populations to environmental conditions. In the past two decades cortisol sequestered in growing hair has received considerable attention in the wildlife, agriculture, and human health fields as a relatively non-invasive means to retrospectively assess mammalian stress (see review by Heimbürge et al. 2019). The concentration of cortisol deposited in the hair matrix (i.e., hair cortisol concentration or HCC) is assumed to be proportional to circulating cortisol. As cortisol is passively deposited in the hair matrix during hair growth, it provides a relatively long-term retrospective view of the conditions experienced by an animal rather than a snapshot of acute stressor events (Heimbürge et al. 2019).

The polar bear (*Ursus maritimus*) is one such species whose conservation can be aided through an understanding of the physiological consequences of life history requirements, seasonal changes in habitat and prey availability, and habitat alternation due to climate change. Although the status of polar bear populations and polar bear health has been tied to the

composition and extent of Arctic sea ice (Bromaghin et al. 2015, Lunn et al. 2016, Regehr et al. 2010, Rode et al. 2010, Stirling et al. 1999), identifying the mechanistic links between population vital rates and the environment has been elusive. However, cortisol that has accumulated in polar bear tissues has promise in linking environmental conditions and polar bear physiology. Because Arctic climate has been warming during the past 30+ years, because polar bears throughout their range undergo cyclical periods of annual prey abundance and scarcity, and because prey consumed varies by polar bear age and sex, cortisol levels likely vary across seasons, among reproductive classes, and through time.

Several studies have examined polar bear HCC with the goal of drawing inferences to environmental conditions (e.g., Bechshøft et al. 2012, 2013, MacBeth et al. 2012, Mislan et al. 2016, Neuman-Lee et al. 2017). Studies have also investigated the relationship between polar bear HCC and reproductive class (Bechshøft et al. 2015, MacBeth et al. 2012, Mislan et al. 2016, Neuman-Lee et al. 2017), body growth and condition (Bechshøft et al. 2015, MacBeth et al. 2012, Mislan et al. 2016), environmental factors (Bechshøft et al. 2013), contaminants (Bechshøft et al. 2012, 2015), and change over time (Bechshøft et al. 2012, Neuman-Lee et al. 2017). The period of primary hair growth in polar bears is assumed to be from approximately May to October (Amstrup 2003, Derocher 2012) and includes the typical season of hyperphagia (late spring and early summer), followed by a season of minimal ice extent (summer through autumn) and food scarcity (Whiteman et al. 2018). Cortisol is passively incorporated into the hair matrix during the active phase of hair growth (Davenport et al. 2006) and hair growth beyond autumn is assumed to be minimal. Hence following autumn, HCC is expected to remain unchanged until the subsequent summer hair molt. Therefore, HCC collected either in the

autumn or spring following hair growth presumably serves as an index on the severity of environmental conditions during the prior minimal ice season.

In this study, we expand on previous research by adding new information from assessments of HCC from polar bears captured in the Beaufort, Bering and Chukchi seas. We compare HCC 1) between autumn and spring in 1983–1989, 2) between three multi-year periods (1983–1989, 2004–2006, and 2008–2016) characterized by highly divergent sea ice conditions (Durner et al. 2009;this study), and 3) among reproductive classes. We also examine the influence of 4) environmental factors and 5) morphometrics and body condition on polar bear HCC.

Methods

Study area and polar bear captures

The U.S. Geological Survey (USGS) captured polar bears in the Alaska portions of the Beaufort (1983–2016), Bering and Chukchi (1987–1997) seas for the purposes of estimating polar bear population size and trend, movements and distribution, habitat relationships, health and nutrition, maternal denning and the response of polar bears to climate-warming driven sea ice declines (e.g., Amstrup et al. 2001, 2010, Atwood et al. 2016, Bromaghin et al. 2015, Durner et al. 2009, Garner et al. 1990, Olson et al. 2017, Pagano et al. 2018, Rode et al. 2020, Whiteman et al. 2015). From 2008 to 2016, the U.S. Fish and Wildlife Service (USFWS) captured polar bears in the Chukchi Sea to address many of the same questions (e.g., Regehr et al. 2018, Rode et al. 2015, Wilson et al. 2016). For both USGS and USFWS research, polar bears were captured by helicopter during searches over sea ice within 160 km of the coast and from logistical bases in Alaska (Fig. 1) including Cape Lisburne, Deadhorse, Kaktovik, Shishmaref, St Lawrence Island, Utqiagvik, Wainwright (USGS), Kotzebue (USGS and USFWS), and the Red Dog Mine Port

(USFWS). Polar bears were immobilized with a projectile syringe, containing sernylan, Phencyclidine, or Etorphine (prior to 1987), or tiletamine hydrochloride plus zolazepam hydrochloride (after 1986; Telazol®, Fort Dodge and Warner-Lambert Co.), fired from a helicopter. USGS captures occurred during spring (March–May) in 1983–1987, 1989, 1991–1993, 1997–2016, and autumn (October and November) in 1981–1986, 1988, 1994, and 1998–2001. Captures by the USFWS were during springs from 2008–2016. We aged bears by 1) visual assessment as dependent young when captured with their mother, or 2) by extracting a vestigial premolar tooth from first capture of independent-aged bears and determining age by analysis of cementum annuli (Calvert and Ramsay 1988). We assigned bears to five age classes: adult (≥5 yr), independent subadult (2–4 years), and dependent 2-year old, yearling, and first-year cubs (i.e., COY).

Sample collection

Between ~0.01 and ~1 g of hair was collected from some captured bears during 1983–1989, 2004–2006, and 2008–2016 (USGS), and 2008–2016 (USFWS). Hair was collected from legs or the rump by either clipping or plucking. MacBeth et al. (2012) found no relationship between polar bear HCC and region of the body where fur was obtained. Hair for each bear was placed in a whirl-pak® plastic bag and frozen at -80° C and later thawed and dried under a laboratory hood at room temperature (~21° C) for ≥ 24 hours. Dried hair samples were weighed with an Ohaus Explorer laboratory balance to subsample hair for cortisol assays. Mean subsample mass was 0.1053 g (std dev = 0.0151, n = 856).

Cortisol assay procedures

Hair samples were prepared and assayed for cortisol by following established methods (Davenport et al. 2006, Macbeth et al. 2010, Neuman-Lee et al. 2017). We first transferred hair samples into 20 ml polypropylene scintillation vials and washed these with 5 ml of HPLC grade

methanol by mixing in a large vortexer for three minutes. Following vortexing we decanted and discarded the waste methanol. This step was repeated until the decanted methanol was clear after washing. After the final wash we placed open vials under a fume hood for 3–5 days to dry the hair. We transferred dried individual samples to a Retsch MM 200 mixer mill (Retsch GmbH, Germany) with a 7 mm steel grinding ball and grinded samples for 20 minutes at 30 hz to convert hair samples to a powder. Powdered hair was then transferred to pre-weighed 5 ml vials (Eppendorf North America, Hauppauge, NY, USA). We then weighed vials with samples to calculate the mass of powdered hair in each vial. We added 3 ml of HPCL grade methanol to each vial and applied paraffin film to vials to ensure that leakage was prevented. Vials were then vortexed vigorously for one minute and then set on a slow vortex for 24 hours. Following this, we vortexed samples for 20 seconds at a rate similar to the first vortexing, and then centrifuged samples for 10 minutes at 2000 rpm. From the centrifuged sample, we decanted the top 1.5 ml of solution and placed this in a clean 12 × 75 mm glass test tube. Samples were dried under nitrogen gas. We resuspended dried samples in either 0.4 ml or 0.5 ml of assay dilutent provided by a commercially available immunoassay kit (Salimetrics, State College, PA, USA). We then vortexed tubes and sealed them by applying a film of paraffin. Test tubes remained undisturbed for ≥ 12 hours to allow the solution to pull cortisol off the walls of the glass. We then performed a final vortex and transferred sample solutions to 2 ml vials. We divided each sample into two 25 µl subsamples and used the immunoassay kit to estimate the cortisol concentration (µg/dL) for each duplicate. Concentration of cortisol in hair was calculated in Excel (Microsoft Excel for Office 365 MSO, version 1908) by 1) first converting the assay concentration to the appropriate units (i.e., µg/dL to pg/mg), 2) dividing the value by the total mass of dried hair used for extractions (mg) to calculate concentration per mg hair weight, and 3) correct for the amount of

extract used in the assay relative to the total resuspension volume of the hair hormone extract (i.e., resultant value multiplied by either 0.5 or 0.4 ml resuspension volume and divided by 0.025 ml used in the assay). The resultant value was pg cortisol per mg polar bear hair, representative of cortisol deposition in hair shaft during the months immediately prior to collection of hair.

Covariates examined to explain HCC

Reproductive class

Samples were assigned to a reproductive class that a bear would have been in the summer prior to the time the sample was collected. This required data on age and, for adult females, observations of dependent young. For autumn-collected hair samples, reproductive status was assigned as the bear's status at the time of sampling (i.e., at year-0). Therefore, males ≥5 years old were assigned AM. Adult females were assigned one of three reproductive classes: 1) solitary (IF), if without young at sampling; 2) with COYs (E0) if accompanied by COYs at sampling; and 3) with yearlings (E1) if accompanied by yearling cubs at sampling. We assumed that IF bears in autumn were solitary throughout the prior summer. It is possible that some IF bears may have been accompanied by young throughout summer and lost those young prior to sampling. Bears were assigned as subadult if their age was 2–4 years; SM and SF for males and females, respectively.

For hair samples collected in spring, HCC was assumed to be a product of conditions during May–October of the prior year. Hence, reproductive class of spring samples was set as the status of the bear at year-1. For example, an adult of age 5 was set as an age 4 subadult because the bear was 4 years old when hair was growing. Similarly, an adult female with 1-year old young when sampled was set as an adult with 0-year old young because the cubs would have been < 1 year old in year-1. Hence, adult females were assigned to one of four reproductive classes: 1) unknown (UF), if captured in the spring without young and no prior data on the

possible status of the bear at year-1; 2) with COYs at year-1 (E0), if captured in the spring with yearling cubs; 3) with yearling cubs at year-1 (E1), if captured in the spring with 2-year old young; and 4) solitary at year-1 (IF), if captured in spring with COYs. Note that with this classification, IF females would have spent the winter prior to sample collection in a maternity den. Adult male (AM) status was assigned when age of a male bear at spring capture was ≥ 6 years; i.e., the bear would have been at least 5 years old during year-1. Subadult status, either SM or SF for male and female bears, respectively, was assigned to bears 2-4 years old. Therefore, bears ≥3 but ≤5 years old captured during spring were assigned subadult status for year-1.

Arctic Oscillation

The Arctic Oscillation (AO) provides an index of the strength and distribution of winds circulating over the Arctic (Proshutinsky et al. 2015, Rigor et al. 2002). Positive phased AO is manifested as relatively low atmospheric sea level within the center Arctic. This results in higher ice drift speeds in the central Arctic Ocean, greater ice divergence along the Asia Arctic Ocean coast, greater spatial extent and strength of the trans polar drift stream and a diminished Beaufort Gyre in both spatial extent and strength. The impact to the Beaufort and Chukchi seas from a positive phased AO is generally expressed by greater ice divergence, reduced retention of multiyear ice, reduced ice thickness, and reduced sea ice extent during the subsequent summer and autumn (Rigor et al. 2002). The Arctic has experienced a greater frequency of positive phase AO since 1989 and at least until 2013 (Proshutinsky et al. 2015, Rigor et al. 2002).

We assessed HCC relative to the mean winter (January–March) AO index provided by the National Oceanographic and Atmospheric Administration's Weather Service, Climate Prediction Centre (http://www.cpc.ncep.noaa.gov/products/precip/CWlink/

daily_AO_index/AO.shtml). A related atmospheric process, the North Atlantic Oscillation NAO), has been linked to HCC fluctuations of Greenland polar bears (Bechshøft et al. 2013). Because the winter AO potentially influences sea ice conditions in the subsequent summer, and summer is the time of most hair growth in polar bears, we assumed that the influence of the AO on HCC in hair samples collected during spring would be due to the previous year's AO (i.e., AO at year-1).

Sea ice

Because polar bears are reliant on sea ice, we derived two indices of summer and autumn sea ice conditions over the Beaufort Sea continental shelf (i.e., ≤300 m deep) that may potentially explain HCC. We used daily sea ice concentration (SIC) derived from 25 × 25 km resolution passive microwave (PM) satellite imagery (National Snow and Ice Data Center [NSIDC], http://nsidc.org/; Cavalieri et al. 1996) to calculate two indices of diminished sea ice over the continental shelf: 1) the open water duration as defined by <15% SIC (OW15); and 2) the open water duration as defined by <50% SIC (OW50). NSIDC considers pixel estimates of SIC <15% as highly uncertain and so these pixels are considered "ice-free" (Overland and Wang 2013). Therefore, we set the annual OW15 period over the Beaufort Sea continental shelf as the first date when >15% of PM pixels over the shelf had <15% sea ice concentration. The end date of each annual OW15 season was marked as the date when <15% of PM pixels had <15% sea ice concentration. Following this same procedure, we also developed an annual OW50 season. We chose this ice concentration threshold because polar bears generally select sea ice concentrations ≥50% (Durner et al. 2009). The OW50 season was set as the duration in days between the first date that >50% of pixels over the Beaufort Sea continental shelf had sea ice concentration <50% and the date that <50% of pixels had sea ice concentration <50%. The duration in days between the first date and the end date was then used as our index of the OW15 and the OW50 seasons,

representative of conditions during the summer and autumn prior to the spring-collected hair samples.

Wind

Wind is a primary driver of sea ice extent, composition and dynamics. Winds associated with storms precondition winter sea ice for summer melting by causing lead formation, increasing proportion of thin new and young ice, and resulting in thermodynamic constraints on ice thickening (Graham et al. 2019). Since 2000 this relationship between wind and sea ice has become more closely coupled as ice has thinned, particularly in the Beaufort and northern Chukchi seas (Spreen et al. 2011). Wind influences sea ice drift, which impacts energetic costs to polar bears (Durner et al. 2017). In addition to the effect of wind on sea ice composition and dynamics, polar bears respond to wind when searching for prey and during migration (Togunov et al. 2017). To assess the role of wind on polar bear hair cortisol levels, we first obtained 10-meter u/v wind data (where u = x-axis and v = y-axis) from the North American Reanalysis (NARR; https://www.ncdc.noaa.gov/data-access/model-data/model-datasets/north-american-regional-reanalysis-narr; accessed September 2019). NARR data are modeled at 3-hr periodicity on a 32-km-resolution grid. We used wind data for January–March and assumed that wind during late winter would influence summer sea ice and therefore polar bear HCC. We selected 11 regularly spaced NARR grid points spanning the Beaufort Sea continental shelf from the Mackenzie River in Canada to Utqiagvik, Alaska. The grid points were aligned roughly parallel with the coast and ~100 km offshore. We first calculated wind speed from the u/v wind components, then calculated daily averages at each grid point. We then averaged the 11 grid points to derive a single daily mean wind speed (WS_MN) and its standard deviation (WS_SD) for the southern Beaufort Sea (SB). The effect of wind on HCC was assessed with wind data from the year prior to spring-collected hair samples.

Polar bear morphometrics

Polar bear morphometrics may be useful predictors of breeding success, cub production, and drawing inferences between nutrition and population dynamics (Rode et al. 2020). Therefore, we explored the relationship between polar bear straight-line body length (SLBL), heart girth (HG), and body mass (M), with HCC. SLBL was measured as the straight-line distance between the tip of the nose and the tip of the last tail vertebra (all 2004–2016 data), or the straight-line distance between the tip of the nose and the base of the tail (all 1983–1989 data), while the immobilized bear was in a sternal recumbent position. To improve consistency of SLBL between 1983–1989 and 2004–2016, we averaged tail length by sex-age class (i.e., subadult males and subadult females, 3–4 years old, AM bears, and females, >5 years old) and added the average tail length to the SLBL for the respective sex-age group in 1983–1989 data. HG was the circumference of the bear's chest immediately behind the bear's forelegs in the sternal recumbent bear. M (kg) was obtained by placing the bear in a cargo net that was connected to a spring-loaded or digital scale, and then raising the net above the surface with a chain hoist suspended from a tripod, or by calculating body mass from morphometrics (e.g., Durner and Amstrup 1996). All morphometrics were normalized by reproductive class so that bears of different age and sex groups could be directly compared.

Time periods

We initially set two major time periods based on when data was collected, 1983–1989 and 2004–2016. This dichotomy was reasonable considering the lapse in years between 1983–1989 and 2004–2016, and that polar bear optimal sea ice habitat had declined substantially from early to the recent period (Durner et al. 2009). However, as explained in the subsequent text, HCC was greater and more variable in 2004–2006 than during other years. Therefore, we examined three time periods, including 1983–1989, 2004–2006, and 2008–2016.

Analysis

We conducted all data preparation and analysis in Program R (The R Foundation for Statistical Computing; ver. 3.5.1). HCC differences between periods, regions, and reproductive classes were first tested for normality and subsequently with a non-parametric analysis of variance (R function *ARTool*) followed by Tukey-corrected multiple comparisons (t-test; R function *emeans*). The relationship between covariates and HCC were explored with general linear models (R function *glm*). Competing general linear models were compared by Akaikie Information Criterion (AIC), delta AIC (ΔAIC), AIC weights (AIC_w), and the significance of covariates. Quadratics and interactions were included in competing models. Two classes of competing models were evaluated; 1) models with environmental covariates; and 2) models with morphometrics. Pearson product correlation (r_p) was used to identify covariates that covaried (R function *cor*). Significance of all statistical tests was set at $p \leq 0.05$.

Results

A total of 517 polar bear hair samples were assayed for HCC. Including all samples, HCC was (mean ± SD) 6.17 ± 5.32 pg mg^{-1} (range: 0.31–36.09). The number of samples among years varied (Table 1) and was uneven between periods and reproductive classes (Table 2). Samples were distributed in the Alaska regions of the Beaufort, Bering and Chukchi seas (Fig. 1). During 1983–1989, there were more samples in spring than autumn for all reproductive classes (there were no autumn samples for 2004–2016; Table 3). Raw data were not normally distributed, and all transformations failed to achieve normality (Shapiro-Wilks test, all $p < 0.001$; supplementary information, Fig. S1). Therefore, we used an Aligned Rank Transformed nonparametric analysis of variance (ANOVA; Wobbrock et al. 2011) in R package "ARTool"

(ver. 0.10.7; https://github.com/mjskay/ARTool) for all subsequent comparisons between seasons, among periods, and among reproductive classes.

Comparing seasons and reproductive classes

Because no autumn samples were available during 2004–2016 tests of seasonal differences in HCC could be performed only with data from 1983–1989. Additionally, spring included seven samples of dependent young (DY; 1st and 2nd year cubs) and 29 samples of adult females of unknown reproductive status (UF), but no samples in these reproductive classes were available in autumn. Therefore, we restricted the comparison between seasons to independent-age polar bears of known reproductive status (n = 182), i.e., subadult females (SF; n = 51), subadult males (SM; n = 26), adult females encumbered with COYs (i.e., E0; n = 34) or encumbered with yearlings (E1; n = 21), solitary adult females (IF; n = 26), and adult males (AM; n = 24). During 1983–1989, HCC in spring (mean ± SD pg mg^{-1}; 4.77 ± 1.58, n = 113) was significantly greater than autumn HCC (3.83 ± 1.04 pg mg^{-1}, n = 69; $F_{1, 170} = 22.564$, $p < 0.001$; Fig. 2). No significant differences in HCC among reproductive classes was apparent in 1983–1989 ($F_{5, 170} = 1.285$, $p = 0.273$) and the interaction between reproductive class and season was not significant ($F_{5, 170} = 1.222$, $p = 0.301$; Fig. 3).

Comparing periods, reproductive classes, and regions

Because HCC was significantly greater in spring than autumn, we excluded autumn from the comparison between periods. Like the comparison between seasons, we excluded dependent young (DY) because there were few samples (n = 11), and adult females of unknown reproductive status (UF; n = 74) because they could not be compared to E0, E1 or IF. Following the exclusion of DY and UF, 363 HCC samples remained for analysis (AM, n = 103; E0, n = 42; E1, n = 34; IF, n = 52; SF, n = 79; SM, n = 53). HCC in 2004–2016 (mean ± SD; 7.54 ± 6.59 pg

mg^{-1}, n = 250) was significantly greater than HCC during 1983–1989 (4.77 ± 1.58 pg mg^{-1}, n = 113; $F_{1, 351} = 9.004$, $p = 0.003$; Fig. 4). However, HCC differences between periods appeared to be driven solely by high HCC during 2004, 2005 and 2006 (Fig. 5, 6; $F_{2, 345} = 21.016$, $p < 0.001$). Therefore, data were binned into three periods for subsequent analyses: 1983–1989, 2004–2006, and 2008–2016. HCC was greater in 2004–2006 (mean ± SD; 11.40 ± 8.62 pg mg^{-1}, n = 101) than 1983–1989 (4.77 ± 1.58 pg mg^{-1}, n = 113; t-ratio = -5.541, $p < 0.001$) and 2008–2016 (4.96 ± 2.48 pg mg^{-1}, n = 149; t-ratio = 6.123, $p < 0.001$; Fig. 6). There was a significant difference among reproductive classes ($F_{5, 345} = 10.358$, $p < 0.001$), and an interaction between reproductive class and period ($F_{10, 345} = 4.464$, $p < 0.001$; Fig. 7). The importance of 2004–2006 in driving the differences among periods and reproductive classes became more evident when the above analysis was repeated with the exclusion of 2004–2006. Differences between 1983–1989 and 2008–2016 were non-significant ($F_{1, 250} = 0.425$, $p = 0.515$), there were no differences among reproductive classes ($F_{5, 250} = 0.969$, $p = 0.437$), and the interaction between reproductive class and period was non-significant ($F_{5, 250} = 2.083$, $p = 0.068$).

Differences in HCC across reproductive classes were due to greater HCC for SF (mean ± SD; 7.84 ± 6.38 pg mg^{-1}) and IF (7.33 ± 6.83 pg mg^{-1}). Subadult females had greater HCC than AM (6.54 ± 5.67 pg mg^{-1}; t-ratio = -3.744, $p = 0.003$), E0 (5.34 ± 3.69 pg mg^{-1}; t-ratio = -5.695, $p < 0.001$), E1 (6.10 ± 5.22 pg mg^{-1}; t-ratio = -4.660, $p = 0.001$), and SM (5.99 ± 4.71 pg mg^{-1}; t-ratio = 4.734, $p < 0.001$). IF bears had greater HCC than E0 (t-ratio = -4.049, $p = 0.001$), E1 (t-ratio = -3.137, $p = 0.023$), and SM (t-ratio = 3.063, $p = 0.028$). Although HCC also was more variable and the mean HCC greater in 2004–2006 for all other reproductive classes (i.e., AM, E0, E1 and SM), mean HCC in 1983-1989 and in 2008–2016 for those reproductive classes always occurred within the 25th and 50th percentiles of 2004–2006 HCC (Fig. 7). A comparison between

AM bears and adult females, including UF bears, found a significant difference in HCC among periods ($F_{2, 299} = 9.912$, $p < 0.001$), but not between sexes ($F_{1, 299} = 1.640$, $p = 0.201$), and a non-significant interaction between sex and period ($F_{2, 299} = 0.094$, $p = 0.911$).

HCC for samples collected during spring in the Beaufort Sea and in the Chukchi Sea (including samples from the Bering Sea) were 7.07 ± 6.27 (n = 274) and 5.48 ± 2.95 (n= 89) pg mg^{-1}, respectively. HCC between regions was not significantly different ($F_{1, 361} = 0.153$, $p = 0.696$).

Relationship between HCC and environmental covariates

A total of 122 models including various combinations of environmental covariates were assessed for their potential to explain polar bear HCC (supplementary information, Table S1). Correlated covariates (i.e., OW15 with OW50, WS_MN with WS_SD; Table 4) were not allowed in the same model. The best model (AIC = 2671.463) included AO, WS_SD, the interaction between AO and WS_SD, OW15, and the quadratic of OW15 (Table 5, S1). The ΔAIC was 8.96, and AIC_w of the best model was 0.99, all of which suggested the top model was superior to all other candidate models (Table 5; see Table S1). All six terms, including the intercept, in the top model were significant (all $p < 0.01$; Table 5, S1).

The top model predicted that HCC responded to the AO and its interaction with the standard deviation of daily wind speed in the Beaufort Sea during January–March (WS_SD; Fig. 8a), and the quadratic of the duration of sea ice extent and concentration <15% (OW15; Fig. 8b). Elevated HCC occurred when the AO was in a positive phase and WS_SD was high (Fig. 8a). However, predicted HCC was low during a positive AO if WS_SD was low, and was low during a negative phase of the AO even when WS_SD was high (Fig. 8a). At both a negative phase AO

and low WS_SD, HCC was predicted to be at levels approximately mid-way between predicted HCC low and high extremes (Fig. 8a).

The predicted response of HCC to the duration of sea ice extent <15% ice concentration (OW15) showed a non-linear response of increasing HCC with increasing OW15 from 0 to approximately 50 days, but then decreasing HCC with OW15 > 50 days (Fig. 8b). Although this pattern is difficult to interpret, predicted HCC relative to OW15 followed a pattern present in the empirical data. Assayed HCC (pg mg^{-1}) at OW15 ≤ 33 days was 4.74 (SD = 1.54, n = 124), at OW15 >33 to < 66 days was 10.49 (SD = 8.72, n = 126), and at OW15 > 66 days was 5.13 (SD = 2.89, n = 187).

Relationship between HCC and morphometrics

Mass (M) was correlated (Table 6) with SLBL (r_p = 0.61) and with HG (r_p = 0.72), hence competing models were reduced to 12 (see Table S2 for results of all models). Body mass (M) and its quadratic (M^2) showed the best explanation for HCC, (Table 7, S2), as it had the lowest AIC (1403.507), the highest AIC_w (0.49), and both βs for the main effect and the quadratic were significant (i.e., $p \leq 0.02$; Table 7, S2). In general, there was a nonlinear and initially abrupt decrease in HCC with increasing body mass of polar bears, with a slight increase in HCC at very high body mass (Fig. 9a). All models including only a single main effect showed a significant negative relationship with HCC, including M (Table S2), HG (Table S2; Fig. 9b), and SLBL (Table S2; Fig. 9c). Most other models had non-significant covariates (Table S2).

Discussion

Our assays of hair cortisol concentration (HCC) from polar bears captured in the Alaska Beaufort, Bering and Chukchi seas suggest that cortisol continues to accumulate in hair from early summer and into the subsequent winter as HCC was greater in spring than autumn. HCC

was greater during 2004–2006 than during either 1983–1989 or 2008–2016, suggesting a physiological response of polar bears to an unidentified environmental perturbation during 2004–2006. Additionally, 2004–2006 coincides with years of reduced survival of SB polar bears. Highly variable HCC in all reproductive classes during 2004–2006 hints that the stress response to during that period affected polar bear demographic groups similarly, although only IF and SF bears showed significantly elevated HCC relative to other reproductive classes. HCC was similar between adult males and adult females. We found no difference in HCC between hair samples collected in the Beaufort Sea, Bering Sea, and Chukchi seas, hence, polar bears across those regions have likely responded similarly to the environmental drivers of HCC. HCC in spring hair samples was elevated following years with a high index winter AO, highly variable winter wind speed, and non-linearly with increasing duration of the summer open water period. There was a negative relationship of HCC with age-specific body mass, body length, and heart girth, indicating that the stress response was more active in smaller bears or bears in or poorer body condition relative to others within their reproductive class.

Comparing seasons and reproductive classes

HCC has shown promise in linking environmental conditions to polar bear physiology, but an important assumption of past studies was that primary hair growth, and hence cortisol deposition in the hair matrix, occurs during late spring to early autumn (Amstrup 2003, Derocher 2012). Our comparison of spring and autumn HCC gives evidence that this assumption may be invalid. This becomes important if comparisons are attempted across polar bear subpopulations, e.g., Hudson Bay (MacBeth et al. 2012, Mislan et al. 2016), Greenland (Bechshøft et al. 2011), and the SB (Newman-Lee et al. 2017, this study), as samples from different seasons may render some comparisons invalid. Hair samples of Western Hudson Bay (WH) polar bears were collected in late summer and early autumn (Bechshøft et al. 2015, MacBeth et al. 2012, Mislan et

al. 2016), while collection season for hair of eastern Greenland polar bears could be across an entire year (Bechshøft et al. 2012). For polar bear hair samples from Alaska, most or all were collected in spring in 1983–1989 and 2004–2016, respectively (Neuman-Lee et al. 2017, this study). Hence, cross-subpopulation comparisons of the stress response via HCC should be made with caution when sample seasons differ among regions.

Comparing periods, reproductive classes, and regions

Our data suggested that spring HCC was elevated in 2004–2006 relative to 1983–1989 and 2008–2016. Different lines of evidence suggest that environmental conditions, physiology, and the behavior of bears have changed in recent years relative to the 1980s. Periods 1983–1989 and 2004–2016 partially coincide with 1985–1996 and 1996–2006, between which annual optimal sea ice habitat the Beaufort and Chukchi seas diminished (Durner et al. 2009), and polar bears were required to obtain more prey to compensate for heightened energetic costs from greater ice drift speed (Durner et al. 2017). Since the late 1990s, the distance between the Alaska-Canada mainland coast and the September ice edge has increased (Pagano et al. 2012), and a greater proportion of both SB and Chukchi Sea polar bears use land during summer and their time on land has increased approximately 30 days (Atwood et al. 2016, Rode et al. 2015). Sea ice declines in recent years have been linked to increase fasting by SB polar bears (Rode et al. 2017, Whiteman et al. 2015), negative impacts to body condition and recruitment (Rode et al. 2010), increased frequency and duration of long-distance swimming (Pagano et al. 2012), and affected their exposure to contaminants and terrestrial pathogens (Atwood et al. 2017, Bourque et al. 2020). Ultimately, declines in sea ice may have negatively impacted the abundance of the SB polar bears (Bromaghin et al. 2015). However, our comparison across years showed that average HCC levels, except for 2004–2006, were unvarying. Elevated and highly variable HCC in 2004–2006 was responsible for differences found between 1983–1989 and 2004–2016. It is

unclear what may have contributed to high HCC during 2004–2006, but interestingly abundance of SB polar bears declined during 2004–2006 (Bromaghin et al. 2015).

Among reproductive classes, IFSF bears had greater HCC than most other classes. The significant interaction between reproductive class and period likely resulted from greater and more variable HCC 2004–2006 than in 1983–1989 and 2008–2016. HCC was greater with SF than AM, E0, E1 and SM bears, and greater with IF than E0, E1, and SM bears. It is notable that our analyses did not identify a difference between AM and adult female bears as was observed by Neuman-Lee et al. (2017). Neuman-Lee et al. (2017) found that HCC was similar between IF bears and those with dependent young. Our analyses showed that IF bears had higher HCC levels than E0 and E1 bears. This apparent discrepancy between Neuman-Lee et al. (2017) and our results, despite both studies using samples collected in the BS, is likely due the temporal brevity of data (i.e., 2013–2015) analyzed by the former study. We found that differences among reproductive classes interacted with period, and 2004–2006 was absent from Neuman-Lee et al. (2017), when polar bears had the highest and most variable HCC levels. Indeed, no differences among reproductive classes would have been observed if 2004–2006 was omitted from this study.

HCC values in this study were largely inconsistent with values reported in other regions. HCC for Alaska polar bears (median = 4.66 pg mg^{-1}, n = 517) was a magnitude greater than for southern Hudson Bay polar bears (median = 0.48 pg mg^{-1}, n = 185; Macbeth et al. 2012) and western Hudson Bay polar bears (median = 0.62 pg mg^{-1}, n = 506; Mislan et al. 2016). For western Hudson Bay polar bears, Mislan et al. (2016) reported elevated HCC in females with dependent young relative to IF bears, but MacBeth et al. (2012) found no difference between these two groups in southern Hudson Bay. Our analyses for samples collected in Alaska

suggested elevated HCC in IF bears during the period of primary hair growth relative to E0 and E1 bears. A possible reason for this difference between our results and those from the Hudson Bay might result from inconsistencies in sampling season, as Hudson Bay samples were collected in autumn and the majority our samples were collected the spring subsequent to the prior summer ice melt season. But even when spring samples were excluded, autumn-collected HCC from Alaska polar bears (median = 3.59 pg mg^{-1}, n = 69) was greater than Hudson Bay samples. As we demonstrated, HCC appears to accumulate during winter. All females coded as IF were known to have been solitary the prior summer because they were observed with COYs when their hair was sampled in spring. Because HCC of IF bears includes the period of maternal den tenure as well as the time of primary hair growth during the prior summer, HCC could also reflect cortisol incorporated into hair during preparation for denning and subsequent time in the maternal den.

Bechshøft et al. (2012) examined HCC from polar bears sampled in eastern Greenland. Unlike studies from Hudson Bay (i.e., MacBeth et al. 2012, Mislan et al. 2016), ~66% of the hair samples examined by Bechshøft et al. (2012) were collected from January to June, and so were more seasonally concordant with our spring hair samples. Bechshøft et al. (2012) showed that HCC of eastern Greenland polar bears (12.8 ± 4.2 pg mg^{-1}, range: 3.98–24.42, n = 88) was twice that of Alaska polar bears (6.17 ± 5.32 pg mg^{-1}, range: 0.31–36.09, n = 517). Similar to our results, Bechshøft et al. (2012) did not detect differences in polar bear HCC between males and females. Unlike the differences in HCC we observed between SF and most other reproductive classes, Bechshøft et al. (2012) did not detect differences between adults and subadults.

Greater HCC in SF bears relative to other reproductive classes was expected. One of the most vulnerable groups of polar bears may be subadults (3–4 years old), as they are recently

weaned, have less efficiency breaking into seal lairs (Stirling and Latour 1978), depend on smaller seals as prey (Thiemann et al. 2011), are subordinate to and potential prey of adult bears (Miller et al. 2015, Stirling and Ross 2011), and their annual survival is typically lower than that of adults (Bromaghin et al. 2015, Regehr et al. 2007). Hence, greater HCC we observed in SF bears relative to most other reproductive classes suggests SF may have experienced greater nutritional stress. SF bears, with a body mass (mean ± SD) of 168.2 ± 26.4 kg (n = 54), were the smallest of all the reproductive classes. In contrast, SM bears were 225.3 ± 61.1 kg (n = 32), and their body mass was surpassed only by AM (376.6 ± 79.6 kg, n = 38). We suggest that SM bears, due to their larger body size, are not prey restricted like SF bears, and this explains the lack of differences in SM HCC compared to other reproductive classes.

We found that IF and SF bears had similar HCC, and greater HCC than E0, E1 and SM bears. In our classification of reproductive status, the months encompassing time as an IF female included breeding, hyperphagia, late summer and early autumn food depravation, and then winter den occupancy. The season of breeding in polar bears begins by late March and may continue until July (Stirling et al. 2016). The duration of interactions between a female and a single male may encompass >14 days, the first seven days of which may involve only non-contact interactions as the two bears become accustomed to one another (Stirling et al. 2016). Because of this, the female may experience physiological stress during the first week of her interactions with the male. Generally, a litter is sired by a single male (Zeyl et al. 2009), hence interactions with other adult males following breeding could be expected to be minimal. The end of the breeding season generally coincides with weaning by ringed and bearded seals, when naïve seal juveniles become available as prey, and during this time pregnant females enter a state of hyperphagia, without the distraction of AM bears or dependent young. Prior to winter, the

body mass of pregnant polar bears may be more than 30% higher than the mass of females accompanied by young (Atkinson and Ramsay 1995). Because all of the adult females classified as IF for year-1 had COYs when they were sampled in spring, they met a minimum weight threshold when they entered the den (Atkinson and Ramsay 1995) and so were unlikely to be nutritionally stressed prior to den entrance. Between autumn and spring, denning polar bears lose ~ 43% of their body mass, and we speculate that this may elicit the stress response. Nutritional stress may continue beyond denning, as adult females with COYs use lower-quality habitats than other reproductive classes (Pilfold et al 2014) and, like subadults, females with COYs have a narrower prey base than adult males (Thiemann et al. 2011). Body mass of IF bears in this study (179.5 ± 23.5 kg, n = 35), sampled during the days or weeks after den departure, was only marginally greater than that of SF bears. Therefore, greater HCC in IF bears may possibly be explained by their tenure in a den, the demands of parturition, nursing, and fasting, and during the weeks following den emergence, reduced use of the most productive hunting habitat (i.e., floe edges and drifting pack) so that they may avoid conspecifics (Johnson and Derocher 2020, Stirling et al. 1993).

Polar bears that inhabit the marine waters of Alaska are largely of the SB and CS subpopulations (Amstrup et al. 2004). The two subpopulations ranges have highly divergent physical and biological oceanography, and different phenology and composition of sea ice. Trends in the dates of spring breakup advancement and delay in autumn freeze-up, and increasing duration of open water, were all ~2× greater in the SB than in the CS during 1979–2014 (Stern and Laidre 2016), resulting in twice as many days of reduced sea ice over the continental shelf in the SB than in the CS (Rode et al. 2014). The CS also has greater biological productively than the SB (Sakshaug 2004). Between recent years and earlier periods, seals in the

CS were reported to be in good body condition and have high reproduction (Crawford et al. 2015), versus declines in condition and reproduction of SB seals during approximately the same periods (Harwood et al. 2015). SB polar bears fast more frequently and are generally of smaller stature and lower body condition than CS polar bears (Rode et al. 2014). Hence, several lines of evidence point towards the SB as potentially more stressful to polar bears than the CS. However, we found no difference in HCC between hair samples collected in the SB versus those collected in the CS and this suggests that the drivers of HCC have been expressed similarly in the CS and the SB.

Relationship between HCC and environmental covariates

The most parsimonious environmental model predicted that HCC was determined by the interaction between the AO and variation in wind speed, and by the quadratic for duration of annual open water season (Fig. 8). The general trend of the winter AO has been towards a high index phase (Proshutinsky et al. 2015), and with that a hemispheric trend of diminished atmospheric pressure resulting in a tendency for Arctic-wide sea ice to drift in a cyclonic (i.e., counterclockwise) versus anti-cyclonic pattern (i.e., low index AO). During a high index AO, the intensity of the Beaufort Gyre and its ability to retain sea ice is reduced, export of sea ice from the Beaufort sea to the East Siberian and Laptev seas is diminished, and export of ice from northern Asia across the North Pole and out of the Arctic through Fram Strait is enhanced (Rigor et al. 2020). A high index winter AO has consequences for polar bear habitat in the Beaufort and Chukchi seas, as winter ice thickness is reduced and surface air temperatures during the following spring may be anomalously high, both of which precondition sea ice for enhanced summer melting (Park et al. 2018, Rigor et al. 2002). Years of low sea level pressure and cyclonic ice drift had generally alternated every 5 to 7 years with periods of high pressure and

anticyclonic ice drift (i.e., low index AO) prior to 1997, but since a high index AO has become the prominent atmospheric mode in the Arctic (Proshutinsky et al. 2015).

A high index AO leads to a greater temporal and spatial extent of open water in the Arctic, which has been linked with negative impacts to polar bear population vital rates (Regehr et al. 2010, Stirling et al. 1999). Similar to our examination of HCC and the AO, HCC from polar bears in eastern Greenland has shown a positive relationship with the NAO (Bechshøft et al. 2013). Like the AO, a negative relationship between the NAO and sea ice extent has been observed (Vinje 2001). The relationship between HCC and the AO (this study) and between HCC and the NAO (Bechshøft et al. 2013) suggests that high index AO and NAO leads to sea ice conditions in the following summer that amplify the polar bear stress response. Interestingly, a positive relationship between ringed seal blubber thickness and the AO was observed in eastern Amundsen Gulf (Harwood et al. 2020), suggesting that the body condition of seal prey trended an opposite path than polar bear HCC during years with a high index winter AO.

We found that the interaction of the AO with variability in wind speed (WS_SD) appeared to influence HCC. Polar bears respond to wind direction so that olfaction-related prey searching is enhanced (Togunov et al. 2017), but the response by polar bears to wind speed and its variation are unknown. WS_SD was positively correlated with wind speed (r_p = 0.90; Table 4), so greater wind speeds may also be partly responsible for elevated HCC. Although our analysis did not identify an interaction between wind speed or its variability with the duration of open water in driving HCC, links between ice concentration and surface winds have been observed. Reduced Arctic ice concentration may be a positive driver of hemispheric and Arctic surface wind speeds (Jakobson et al. 2019, Kennel and Yulaeva 2020). Hence, the relationship between wind variability and speed with HCC that we identified may be a proxy for underlying

sea ice conditions that were not considered in our suite of environmental covariates, and that those sea ice covariates may also influence polar bear HCC.

We found a nonlinear relationship between HCC and duration of sea ice concentration <15% over the continental shelf (OW15). HCC increased from zero days to approximately 50 days OW15, and then decreased after 50 days to a level nearly that of HCC at zero days OW15. The observed decrease in HCC with increasing duration of open water beyond 50 days was unexpected, because a negative relationship of polar bear body condition with increasing duration of summer open water has been observed (Rode et al. 2010), and HCC is linked to polar bear body condition (this study, MacBeth et al. 2012). A potential explanation for this apparent contradiction involves ringed seal productivity relative to the timing of breakup and the duration and extent of the summer open water season. Reproduction and recruitment of ringed seals has been linked to spring sea ice conditions, as the proportion of the ringed seal subsistence harvest that is composed of juveniles and the ovulation rates of harvested adult females were both positively linked to advancement of spring breakup in eastern Amundson Gulf (Harwood et al. 2020). Therefore, it is plausible that some advancement of breakup, and prolonged open water, as defined by < 15% sea ice concentration, may benefit polar bears by increasing the availability of juvenile seals as prey. Although sea ice >50% concentration appears optimal for polar bears (Durner et al. 2009), polar bears may continue to occupy suboptimal sea ice for days to weeks before moving to other habitats (Cherry et al. 2016, McCall et al. 2016). Use of suboptimal sea ice coupled with early breakup and boost of juvenile seal abundance may benefit polar bears and reduce expression of the stress response. However, if this relationship is true, it is expressed when OW15 increases beyond 50 days. Why this threshold of >50 days appears in our data is for reasons that we cannot explain.

Relationship between HCC and morphometrics

Our analysis suggests that polar bear HCC was a function of body size (normalized by reproductive class; Fig. 9). This relationship was best explained with polar bear body mass (M) but was also evident with SLBL and HG, all of which were correlated so combinations of these covariates could not be included in the same model. M with its quadratic was the best predictive model as AIC_w was highest among models and both terms were significant (Table 7, S2). As M increased there was a non-linear decrease of HCC (Fig. 9a). HCC decreased with increasing SLBL (Fig. 9b) and with increasing HG (Fig. 9c), indicating that these covariates, when used alone, were also predictive of polar bear HCC. Our results are consistent with the conclusions of other studies that have examined HCC relative to body condition in polar bears and other species of bears (Cattet et al. 2014, MacBeth et al. 2012, Mislan et al. 2016, Neuman-Lee et al. 2017). In general, and within their respective reproductive classes, heavier and larger polar bears had lower HCC.

Conclusions and Management Implications

Our investigation of cortisol in the hair of polar bears that use the Beaufort, Bering and Chukchi seas near Alaska bring forth several lines of evidence that can serve the information needs of resource managers and future research. We have shown that cortisol continues to accumulate in polar bear hair throughout winter. Therefore, comparisons of the stress response across subpopulations should be made when sample collection seasons are similar. We show that HCC responded positively with increasing winter Arctic Oscillation index and with increasing variation of wind speed. As a positive AO becomes more frequent and if wind speeds become more variable in response to decreased sea ice, conditions that elicit the stress response in polar bears will likely increase in intensity and frequency. Our analysis suggests that the

temporal and spatial extent of ice-free waters over the continental shelf also influenced HCC, increasing with open water, but decreasing beyond an open water threshold of 50 days duration. The decrease in HCC relative to a 50-day open water threshold may be due to seal prey becoming more available to bears.

Polar bear HCC was related to body condition. Within their reproductive class, larger and heavier polar bears had lower HCC than smaller bears. But we also found differences among reproductive classes. Adult female polar bears with COYs, who were solitary the prior year (IF), and subadult females (SF), had greater HCC than most other reproductive classes. Greater HCC, coupled with the lowest body mass of all reproductive classes, suggests that IF and SF bears may have greater vulnerability to environmental perturbations than other polar bears.

Finally, our analyses identified HCC in 2004–2006 as anomalously high and variable relative to all other years. Across reproductive classes, HCC of IF and SF bears in 2004–2006 was greater than most other reproductive classes during 2004–2006, and in 1983–1989 and 2008–2016. However, HCC of all reproductive classes in 2004–2006 was highly variable relative to other time periods. This suggests that perturbations leading to and including 2004–2006 impacted all polar bears, regardless of reproductive class. That perturbation has not been identified, but it and resulting HCC levels may be a link to measured reduced survival and abundance of SB polar bears during 2004–2006 (Bromaghin et al. 2015). Because we found no difference in HCC among regions, the health and population status of polar bears in the Bering and Chukchi seas may also have been impacted during 2004–2006.

Our research points to the value of long-term and consistent investigations of an Arctic apex predator. Had our data excluded several key years then our results and conclusions may have had a different outcome. Future research should further clarify the mechanistic links

between the environment and polar bear health and population status. Conservation efforts by the USFWS for polar bear populations in the United States are directed toward maintaining viable populations despite climate-driven sea ice loss (USFWS 2016). Our results can be used to inform conservation as we provide additional evidence that certain demographic groups may be more vulnerable than others. Coupled with recent demographic analyses of SB polar bears (Atwood et al. 2020), our results also suggest that environmental perturbations within the span of several years may lead to significant population-wide effects on polar bear health, with possible impacts to population status and trend.

Acknowledgements

This research was supported by the U.S. Geological Survey (USGS) and by the North Pacific Research Board (project numbers 1716A and 1716B). Additional support was provided by the USGS Changing Arctic Ecosystems Initiative; U.S. Fish and Wildlife Service (USFWS), Marine Mammals Management, and the Arctic National Wildlife Refuge; the U.S. Bureau of Land Management; the North Slope Borough, Department of Wildlife Management; the Polar Continental Shelf Project; and the University of Wyoming (National Science Foundation grant: OPP 0732713). This research was permitted under the Marine Mammal Protection Act and Endangered Species Act under permit MA690038 (USGS) and MA046081 (USFWS) and followed protocols approved by Animal Care and Use Committee of the USGS (assurance no. 2010–3) and the USFWS Alaska Regional Office Animal Care and Use Committee. We thank the numerous biologists and pilots whose efforts were essential for capturing and sampling polar bears. Cortisol assays were conducted by the French Laboratory, Department of Biology, Utah State University. We thank Cody McIntyre and Vanessa Muhlenbruch for assistance in the laboratory. We thank Andrew Reeves, Sarah Laske and John Pearce for their constructive input

on prior versions of this manuscript. This report has been peer reviewed and approved for publication consistent with USGS Fundamental Science Practices (https://pubs.usgs.gov/circ/1367/). Any use of trade, firm, or product names is for descriptive purposes only and does not imply endorsement by the U.S. Government. The authors claim that they have no conflict of interest. Data used in this report will be available after a 2-year embargo following the publication of this report. Data and metadata may be obtained in Durner (2020; https://doi.org/10.5066/P9RP5KJP), through the North Pacific Research Board (projects 1716A and 1716B; https://www.nprb.org/), and DataOne (https://www.dataone.org/).

Literature

Amstrup, S.C. 2003. The polar bear, *Ursus maritimus*. Pages 587–610 in G. C. Feldhamer, B.C. Thompson, and J.A. Chapman, editors. Wild mammals of North America: biology, management and conservation. John Hopkins University Press, Baltimore, Maryland, USA.

Amstrup, S.C., E.T. DeWeaver, D.G. Douglas, B.G. Marcot, G.M. Durner, C.M. Bitz, and D.A. Bailey. 2010. Greenhouse gas mitigation can reduce sea-ice loss and increase polar bear persistence. Nature, 468:955–958. doi.org:10.1038/nature09653.

Amstrup, S.C., G.M. Durner, T.L. McDonald, D.M. Mulcahy, and G.W. Garner. 2001. Comparing movement patterns of satellite-tagged male and female polar bears. Canadian Journal of Zoology, 79:2147–2158. doi.org: 10.1139/cjz-79-12-2147.

Atkinson, S.N., and M.A. Ramsay. 1995. The effects of prolonged fasting of the body composition and reproductive success of female polar bears (*Ursus maritimus*). Functional Ecology, 9:559–567.

Atwood, T.C., J.F. Bromaghin, V.P. Patil, G.M. Durner, D.C. Douglas, and K.S. Simac. 2020 Analyses on subpopulation abundance and annual number of maternal dens for the U.S. Fish and Wildlife Service on polar bears (*Ursus maritimus*) in the southern Beaufort Sea, Alaska: U.S. Geological Survey Open-File Report 2020-1087, 16 p., https://doi.org/10.3133/ofr20201087.

Atwood, T.C., C. Duncan, K.A. Patyk, P. Nol, J. Rhyan, M. McCollum, M.A. McKinney, A.M. Ramey, C.K. Cerqueira-Cézar, O.C.H. Kwok, J. Dubey, and S. Hennager. 2017. Environmental and behavioral changes may influence the exposure of an Arctic apex

predator to pathogens and contaminants. Nature, 7:13193. Doi.org: 10.1038/s41598-017-13496-9.

Atwood, T. C., E. Peacock, M. A. McKinney, K. Lillie, R. Wilson, D. C. Douglas, S. Miller, and T. Terletzky. 2016. Rapid environmental change drives increased land use by an Arctic marine predator. PLoS ONE, 11: doi:10.1371/journal.pone.0155932.

Barcellos, L.J.G., A. Marqueze, M. Trapp, R.M. Quevedo, and D. Ferreira. 2010. The effects of fasting on cortisol, blood glucose and liver and muscle glycogen in adult jundiá *Rhamdia quelen*. Aquaculture, 300:231–236.

Bechshoft, T., A.E. Derocher, E. Richardson, E. P. Mislan, N. J. Lunn, C. Sonne, R. Dietz, D. M. Janz, and V. L. St. Louis. 2015. Mercury and cortisol in Western Hudson Bay polar bear hair. Ecotoxicology, 24:1315–1321, doi:10.1007/s10646-015-1506-9.

Bechshøft, T. Ø., C. Sonne, R. Dietz, E.W. Born, M.A. Novak, E. Henchey, and J.S. Meyer. 2011. Cortisol levels in hair of East Greenland polar bears. Science of the Total Environment, 409:831-834.

Bechshøft, T. Ø., C. Sonne, R. J. Letcher, D. C. G. Muir, M. A. Novak, E. Henchey, J. S. Meyer, I. Eulaers, V. L. B. Jaspers, M. Eens, A. Covaci, and R. Dietz. 2012. Measuring environmental stress in East Greenland polar bears, 1982–1927 and 1988–2009: What does hair cortisol tell us? Environment International 45: 15–21.

Bechshøft, T. Ø., C. Sonne, F. F.Rigét, R. J. Letcher, M. A. Novak, E. Henchey, J. S. Meyer, I. Eulaers, V. L. B. Jaspers, A. Covaci, and R. Dietz. 2013. Polar bear stress hormone cortisol fluctuates with the North Atlantic Oscillation climate index. Polar Biology 36: 1525–1529.

Boonstra, R. 2004. Coping with changing northern environments: the role of the stress axis in birds and mammals. Integr. Comp. Biol., 44:95–108.

Bourque, J., J.-P. Desforges, M. Levin, T.C. Atwood, C. Sonne, R. Deitz, T.H. Jensen, E. Curry, and M.A. McKinney. 2020. Climate-associated drivers of plasma cytokines and contaminant concentrations in Beaufort Sea polar bears (*Ursus maritimus*). Science of the Total Environment (2020), https://doi.org/10.1016/j.scitotenv.2020.140978.

Braun, T.P., and D.L. Marks. 2015. The regulation of muscle mass by endogenous glucocorticoids. Frontiers in Physiology, 6(12), doi:10.3389/fphys.2015.00012.

Bromaghin, J.F., McDonald, T.L., Stirling, I., Derocher, A.E., Richardson, E.S., Regehr, E.V., Douglas, D.C., Durner, G.M., Atwood, T., and Amstrup, S.C. 2015. Polar bear population dynamics in the southern Beaufort Sea during a period of sea ice decline. Ecological Applications 25: 634–651. doi: 10.1890/14-1129.1.

Cattet, M., B.J. Macbeth, D.M. Janz, A. Zedrosser, J.E. Swenson, M. Dumond, and G.B. Stenhouse. 2014. Quantifying long-term stress in brown bears with the hair cortisol concentration: a biomarker that may be confounded by rapid changes in response to capture and handling. Conservation Physiology, 2. Doi:10.1093/conphys/cou026

Cavalieri, D. J., C. L. Parkinson, P. Gloersen, and H. Zwally. 1996 (updated continually). Sea ice concentrations from Nimbus-7 SMMR and DMSP SSM/I-SSMIS passive microwave data. NASA National Snow and Ice Data Center Distributed Active Archive Center, Boulder, Colorado, USA.

Cherry, S.G., A.E. Derocher, and N.J. Lunn. 2016. Habitat-mediated timing of migration in polar bears: an individual perspective. Ecology and Evolution, 6:5032–5042. doi: 10.1002/ece3.2233.

Crawford, J.A., L.T. Quakenbush, and J.J. Citta. 2015. A comparison of ringed and bearded seal diet, condition and productivity between historical (1975–1984) and recent (2003–2012) periods in the Alaskan Bering and Chukchi seas. Progress in Oceanography, 136:133–150. http://dx.doi.org/10.1016/j.pocean.2015.05.011.

Davenport, M.D., S. Tiefenbacher, C.K. Lutz, M.A. Novak, and J.S. Meyer. 2006. Analysis of endogenous cortisol concentrations in the hair of rhesus macaques. General and Comparative Endocrinology, 147:255–261, doi:10.1016/j/y/gcen.2006.01.005.

de Quervain, D.J.-F., B. Roozendaal, and J.L. McGaugh. 1998. Stress and glucocorticoids impair retrieval of long-term spatial memory. Nature, 394:787–790.

Derocher, A.E. 2012. Polar Bears: A Complete Guide to Their Biology and Behavior. The Johns Hopkins University Press, Baltimore, Maryland.

Durner, G.M., and S.C. Amstrup. 1996. Mass and body-dimension relationships of polar bears in northern Alaska. Wildlife Society Bulletin, 24(3): 480–484.

Durner G.M., Douglas D.C., Nielson R.M., Amstrup S.C., McDonald T.L., Stirling I., Mauritzen M., Born E.W., Wiig Ø., DeWeaver E., Serreze M.C., Belikov S.E., Holland M.M., Maslanik J., Aars J., Bailey D.A. and Derocher A.E. 2009. Predicting 21st-century polar bear habitat distribution from global climate models. Ecological Monographs 79, 25–58.

Durner, G. M., D. C. Douglas, S. E. Albeke, J. P. Whiteman, M. Ben-David, S. C. Amstrup, E. Richardson, and R. R. Wilson. 2017. Increased Arctic sea ice drift alters adult female polar bear movements and energetics. Global Change Biology 23:3460–3473.

Durner, G.M. 2020. Data from polar bear hair samples assayed for cortisol and collected in the Bering, Chukchi, and Beaufort seas, Alaska, 1983-1989 and 2004-2016. U.S. Geological Survey data release, https://doi.org/10.5066/P9RP5KJP.

Garner, G.W., S.T. Knick, and D.C. Douglas. 1990. Seasonal movements of adult female polar bears in the Bering and Chukchi seas. Bears: Their Biology and Management, 8:219–226. http://www.jstor.org/stable/3872922.

Gentsch, R.P., P. Kjellander, and B.O. Röken. 2018. Cortisol response of wild ungulates to trauma situations: hunting is not necessarily the worst stressor. European Journal of Wildlife Research, 64(11), doi:10.1007/s10344-018-1171-4.

Graham, R.M. et al. 2019. Winter storms accelerate the demise of sea ice in the Atlantic sector of the Arctic Ocean. Nature Scientific Reports, 9:9222. doi.org/10.1038/s41598-019-45574-5.

Harwood, L.A., T.G. Smith, J.C. George, S.J. Sandstrom, W. Walkusz, and G.J. Divoky. 2015. Change in the Beaufort Sea ecosystem: Diverging trends in body condition and/or production in five marine vertebrate species. Progress in Oceanography, 136:263–273.

Heimburge, S., E. Kanitz, and W. Otten. 2019. The use of hair cortisol for the assessment of stress in animals. General and Comparative Endocrinology, 270:10–17, doi:10.1016/j.ygcen.2018.09.016.

Hontela, A., J.B. Rasmussen, C. Audet, and G. Chevalier. 1992. Impaired cortisol stress response in fish from environments polluted by PAHs, PCBs, and mercury. Archives of Environmental Contamination and Toxicology, 22:278–283, doi:10.1007/BF00212086.

Jakobson, L., T. Vihma, and E. Jakobson. 2019. Relationships between sea ice concentration and wind speed over the Arctic Ocean during 1979–2015. Journal of Climate, 32:7783–7796. DOI: 10.1175/JCLI-D-19-0271.1.

Johnson, A.M., and A.E. Derocher. 2020. Variation in habitat use of Beaufort Sea polar bears. Polar Biology, 43:1247–1260. Doi.org:10.1007/s00300-020-02705-3.

Kennel, C.F., and E. Yulaeva. 2020. Influence of Arctic sea-ice variability on Pacific trade winds. Proceedings of the National Academy of Science, 117:2824–2834. doi.org/10.1073/pnas.1717707117.

Kirby, E.D., A.C. Geraghty, T. Ubuka, G.E. Bentley, and D. Kaufer. 2009. Stress increases putative gonadotropin inhibitory hormone and decreases luteinizing hormone in male rats. Proceedings of the National Academy of Science, 106(27):11,324–11,329, doi:10.1073_pnas.0901176106.

Lunn, N.J., Servanty, S., Regehr, E.V., Converse, S.J., Richardson, E., and Stirling, I. 2016. Demography of an apex predator at the edge of its range: impacts of changing sea ice on polar bears in Hudson Bay. Ecological Applications, 26: 1302–1320. doi.org/10.1890/15-1256.

Macbeth, B. J., M. R. L. Cattet, M. E. Obbard, K. Middel, and D. M. Janz. 2012. Evaluation of hair cortisol concentration as a biomarker of long-term stress in free-ranging polar bears. Wildlife Society Bulletin doi:10.1002/wsb.219.

McCall, A.G., N.W. Pilfold, A.E. Derocher, and N.J. Lunn. 2016. Seasonal habitat selection by adult female polar bears in western Hudson Bay. Population Ecology, 58:407–419. doi.org/10.1007/s10144-016-0549-y.

Miller, S., J. Wilder, and R.R. Wilson. 2015. Polar bear-grizzly bear interactions during the autumn open-water period in Alaska. Journal of Mammalogy, 96:1317–1325. http://www.bioone.org/doi/full/10.1093/jmammal/gyv140.

Mislan, P., A. E. Derocher, V. L. St. Louis, E. Richardson, N. J. Lunn, and D. M. Janz. 2016. Assessing stress in Western Hudson Bay polar bears using hair cortisol concentration as a biomarker. Ecological Indicators 71: 47–54.

Morey, J.N., I.A. Boggero, A.B. Scott, and S.C. Segerstrom. 2015. Current directions in stress and human immune function. Current Opinion in Psychology, 5:13–17, doi: 10.1016/j.copsyc.2015.03.007.

Nakamura, Y., B.R. Walker, and T. Ikuta. 2016. Systematic review and meta-analysis reveals acutely elevated plasma cortisol following fasting but not less severe calorie restriction. Stress, 19(2):151–157, doi:10.3109/10253890.2015.1121984.

Narayan, E. 2019. Physiological stress levels in wild koala sub-populations facing anthropogenic induced environmental trauma and disease. Scientific Reports, 9:6031, doi: 10.1038/s41598-019-42448-8.

Neuman-Lee, L.A., P.A. Terletzhy, T.C. Atwood, E.M. Gese, G.D. Smith, S. Greenfield, J. Pettit, and S.S. French. 2017. Demographic and temporal variations in immunity and condition of polar bears (*Ursus maritimus*) from the southern Beaufort Sea. Journal of Experimental Zoology, 327(5): 333–346, doi:10.1002/jez.2112.

Olson, J., K.D. Rode, D. Eggett, T.S. Smith, R.R. Wilson, G.M. Durner, A.S. Fischbach, T. C. Atwood, and D.C. Douglas. 2017. Identifying maternal denning of polar bears using temperature—Denning substrate in relation to sea ice in the southern Beaufort Sea. Marine Ecology Progress Series, 564:211−224.

Ortiz, R.M., C.E. Wade, and C.L. Ortiz. 2001. Effects of prolonged fasting on plasma cortisol and TH in postweaned northern elepahnt seal pups. American Journal of Physiology-Regulatory, Integrative and Comparative Physiology, 280:R790–R795, doi: 10.1152/ajpregu.2001.280.3.R790.

Overland, J. E., and M. Wang. 2013. When will the summer Arctic be nearly ice free? Geophysical Research Letters 40:2097−2101.

Pagano, A.M., G.M. Durner, S.C. Amstrup, K.S. Simac, and G.S. York. 2012. Long-distance swimming by polar bears (*Ursus maritimus*) of the southern Beaufort Sea during years of extensive open water. Canadian Journal of Zoology, 90:663–676. doi:10.1139/Z2012-033.

Pagano, A.M., G.M. Durner, K.D. Rode, T.C. Atwood, S.N. Atkinson, E. Peacock, D.P. Costa, M.A. Owen, and T.M. Williams. 2018. High-energy, high-fat lifestyle challenges an Arctic apex predator, the polar bear. Science, 359: 568–572.

Park, H., A.L. Stewart, and J. Son. 2018. Dynamic and thermodynamic impacts of the winter Arctic Oscillation on summer sea ice extent. Journal of Climate, 31:1483–1497. doi.org:10.1175/JCLI-D-17-0067.1.

Pearson, B.L., D.M. Reeder, and P.G. Judge. 2015. Crowding increases salivary cortisol but not self-directed behavior in captive baboons. American Journal of Primatology, 77(4):462–467, doi: 10.1002/ajp.22363.

Pilfold, N.W., A.E. Derocher, and E. Richardson. 2014. Influence of intraspecific competition on the distribution of a wide-ranging, non-territorial carnivore. Global Ecology and Biogeography, 23:425–435

Proshutinsky, A., D. Dukhovskoy, M. L. Timmermans, R. Krishfield, and J. L. Bamber. 2015. Arctic circulation regimes. Philosophical Transactions of the Royal Society-A 373: 20140160, doi:10.1098/rsta.2014.0160.

Regehr E.V., N.J. Hostetter, R.R. Wilson, K.D. Rode, M. St. Martin, and S.J. Converse. 2018. Integrated population modeling provides the first empirical estimates of vital rates and abundance for polar bears in the Chukchi Sea. Nature, 8:16780. doi.org:10.1038/s41598-018-34824-7.

Regehr, E. V., C. M. Hunter, H. Caswell, S. C. Amstrup, and I. Stirling. 2010. Survival and breeding of polar bears in the southern Beaufort Sea in relation to sea ice. Journal of Animal Ecology 79:117–127.

Regehr, E.V., N.J. Lunn, S.C. Amstrup, and I. Stirling. 2007. Effects of earlier sea cie breakup on survival and population size of polar bears in western Hudson Bay. The Journal of Wildlife Management, 71:2673–2683. 10.2193/2006-180.

Rich, E.L., and L.M. Romero. 2005. Exposure to chronic stress downregulates corticosterone responses to acute stressors. American Journal of Physiology-Regulatory, Integrative and Comparative Physiology, 288: R1628–R1636, doi:10.1152/ajpregu.00484.2004.

Rode, K.D., S.C. Amstrup, and E.V. Regehr. 2010. Reduced body size and cub recruitment in polar bears associated with sea ice declines. Ecological Applications, 20:768–782.

Rode, K.D., T.C. Atwood, G.W. Thiemann, M. St. Martin, R.R. Wilson, G.M. Durner, E.V. Regehr, S.L. Talbot, G.K. Sage, A.M. Pagano, and K. Simac. 2020. Identifying reliable indicators of fitness in polar bears. PLoS ONE, 15: e0237444. doi.org:10.1371/journal.pone.0237444.

Rode, K.D., E.V. Regehr, D.C. Douglas, G. Durner, A.E. Derocher, G.W. Thiemann, and S.M. Budge. 2014. Variation in the response of an Arctic top predator experiencing habitat loss: feeding and reproductive ecology of two polar bear populations. Global Change Biology, 20:76–88. doi: 10.1111/gcb.12339.

Rode, K.D., R.R. Wilson, D.C. Douglas, V. Muhlenbruch, T.C. Atwood, E.V. Regehr, E.S. Richardson, N.W. Pilfold, A.E. Derocher, G.M. Durner, I. Stirling, S.C. Amstrup, M. St. Martin, A.M. Pagano, and K. Simac. 2017. Spring fasting behavior in a marine apex predator provides an index of ecosystem productivity. Global Change Biology, 2017. doi.org:10.1111/gcb.13933.

Rode, K.D., R.R. Wilson, E.V. Regehr, M. St. Martin, D.C. Douglas, and J. Olson. 2015 Increased land use by Chukchi Sea polar bears in relation to changing sea ice conditions. PLoS ONE, 10: e0142213. doi:10.1371/journal.pone.0142213.

Sakshaug, E. 2004. Primary and secondary production in the Arctic Seas. Pages 57–81 in R. Stein and R.W. MacDonald (eds): The Organic Carbon Cycle in the Arctic Ocean. Springer, Berlin.

Sapolsky, R.M., L.M. Romero, and A.U. Munck. 2000. How do glucocorticoids influence stress responses? Integrating permissive, suppressive, stimulatory, and preparative actions. Endocrine Reviews, 21(1):55–89.

Schliebe, S., K.D. Rode, J.S. Gleason, J. Wilder, K. Proffitt, T.J. Evans, and S. Miller. 2008. Effects of sea ice extent and food availability on spatial and temporal distribution of polar bears during the fall open-water period in the Southern Beaufort Sea. Polar Biology, 31:999–1010. DOI 10.1007/s00300-008-0439-7.

Stern, H.L., and K.D. Laidre. 2016. Sea-ice indicators of polar bear habitat. The Cryosphere, 10: 2027–2041. doi:10.5194/tc-10-2027-2016.

Smith, S.M., and W.W. Vale. 2006. The role of the hypothalamic-pituitary-adrenal axis in neuroendocrine responses to stress. Dialogues in Clinical Neuroscience, 8(4):383–395.

Spreen, G., R. Kwok, and D. Menemenlis. 2011. Trends in Arctic sea ice drift and role of wind forcing: 1992–2009. Geophysical Research Letters, 38: doi:10.1029/2011GL048970.

Stirling, I., D. Andriashek, and W. Calvert. 1993. Habitat preferences of polar bears in the western Canadian Arctic in later winter and spring. Polar Record, 29:13–24.

Stirling, I., and P.B. Latour. 1978. Comparative hunting abilities of polar bear cubs of different ages. Canadian Journal of Zoology, 56:1768–1772.

Stirling, I., N.J. Lunn, and J. Iacozza. 1999. Long-term trends in the population ecology of polar bears in Western Hudson Bay in relation to climatic change. Arctic, 52:294–306.

Stirling, I., and J.E. Ross. 2011. Observations of cannibalism by polar bears (*Ursus maritimus*) on summer and autumn sea ice at Svalbard, Norway. Arctic, 64:478–482.

Stirling, I., C. Spencer, and D. Andriashek. 2016. Behavior and activity budgets of wild breeding polar bears (*Ursus maritimus*). Marine Mammal Science, 32:13–37. Doi.org: 10.1111/mms.12291.

Stirling, I., G. W. Thiemann, and E. Richardson. 2008. Quantitative support for a subjective fatness index for immobilized polar bears. Journal of Wildlife Management, 72:586–574, doi:10.2193/2007-123.

Thiemann, G.W., S.J. Iverson, I. Stirling, and M.E. Obbard. 2011. Individual patterns of prey selection and dietary specialization in an Arctic marine carnivore. Oikos, 120: 1469–1478. Doi.org:10.1111/j.1600-0706.2011.19277.x.

Tilbrook, A.J., A.I. Turner, and I.J. Clarke. 2000. Effects of stress on reproduction in non-rodent mammals: the role of glucocorticoids and sex differences. Reviews of Reproduction, 5:105–113.

Togunov, R.R., A.E. Derocher, and N.J. Lunn. 2017. Windscapes and olfactory foraging in a large carnivore. Nature, 7:46332. doi.org: 10.1038/srep46332.

Turnlund, J., S. Margen, and G.M. Briggs. 1979. Effect of glucocorticoids and calcium intake on bone density and bone, liver and plasma minerals in Guinea pigs. Journal of Nutrition, 109(7):1175–1188, doi:10.1093/jn/109.7.1175.

USFWS. 2016. Polar Bear (*Ursus maritimus*) Conservation Management Plan, Final. U.S. Fish and Wildlife, Region 7, Anchorage, Alaska. 104 pp. https://www.adaptationclearinghouse.org/resources/usfws-polar-bear-conservation-management-plan.html, accessed 27 May 2020.

Vinje, T. 2001. Anomalies and trends of sea-ice extent and atmospheric circulation in the Nordic seas during the period 1864–1998. Journal of Climate, 14:255–267.

Whiteman, J.P., H.J. Harlow, G.M. Durner, R. Anderson-Sprecher, S.E. Albeke, E.V. Regehr, S.C. Amstrup, and M. Ben-David. 2015. Summer declines in activity and body temperature offer polar bears limited energy savings. Science, 349:295–.298. doi: 10.1126/science.aaa8623.

Whiteman, J.P., H.J. Harlow, G.M. Durner, E.V. Regehr, S.C. Amstrup, and M. Ben-David. 2018. Phenotypic plasticity and climate change: can polar bears respond to longer Arctic summers with an adaptive fast? Oecologia, 186:369–381.

Whitworth, J.A., P.M. Williamson, G. Mangos, and J.J. Kelly. 2005. Cardiovascular consequences of cortisol excess. Vascular Health Risk Management, 1(4):291–299, doi:10.2147/vhrm.2005.1.4.291.

Wilson, R.R., and G.M. Durner. 2020. Seismic survey design and effects on maternal polar bear dens. Journal of Wildlife Management, 84:201−212.

Wobbrock, J.O., L. Findlater, D. Gergle, and J.J. Higgins. 2011. The Aligned Rank Transform for nonparametric factorial analyses using only ANOVA procedures. Proceedings of the ACM Conference on Human Factors in Computing Systems (CHI ’11). Vancouver, British Columbia (May 7–12, 2011). New York: ACM Press, pp. 143–146, doi:10.1145/1978942.1978963.

Zeyl, E., J. Aars, D. Ehrich, L. Bachmann, and O. Wiig. 2009. The mating system of polar bears: a genetic approach. Canadian Journal of Zoology, 87:1195–1209. doi.org:10.1139/Z09-107.

Tables

Table 1. Number of polar bear hair samples assayed for cortisol by year and reproductive class during the season when cortisol was incorporated in the hair (n = 517). AM = adult (≥ 5 years old) male, UF = adult female of unknown status, EF = adult female with dependent young, IF = adult female without young, DY = dependent young (0–1 years old), SF = subadult (2–4 years old) female, SM = subadult male.

year	AM	DY	EF	IF	SF	SM	UF
1983	8	3	7	2	15	8	5
1984	5	1	10	6	7	4	5
1985	5	1	5	6	12	5	3
1987	3	0	4	0	4	3	4
1988	3	2	28	8	12	6	10
1989	0	0	1	4	1	0	2
2004	28	0	11	11	17	7	8
2005	2	0	1	1	0	0	0
2006	14	0	3	1	4	1	3
2008	2	0	1	5	5	1	12
2009	7	0	3	4	3	4	6
2010	2	0	6	4	1	0	4
2011	4	0	2	0	1	6	0
2013	13	1	5	4	7	8	7
2014	9	3	3	3	10	6	3
2015	1	0	0	0	0	0	0
2016	5	0	10	0	2	2	2

Table 2. Number of polar bear hair samples assayed for cortisol, 1983–1989 and 2004–2016 by reproductive class during the season when cortisol was incorporated in the hair. AM = adult (≥ 5 years old) male, UF = adult female of unknown status, EF = adult female encumbered by dependent young, IF = adult female without young, DY = dependent young (0–1 years old), SF = subadult (2–4 years old) female, SM = subadult male.

period	AM	DY	EF	IF	SF	SM	UF
1983–1989	24	7	55	26	51	26	29
2004–2016	87	4	45	33	50	35	45

Table 3. Number of polar bear hair samples assayed for cortisol for spring and autumn by reproductive class in 1983–1989 (there were no autumn samples in 2004–2016). AM = adult (≥ 5 years old) male, UF = adult female of unknown status, EF = adult female encumbered by dependent young, IF = adult female without young, DY = dependent young (0–1 years old), SF = subadult (2–4 years old) female, SM = subadult male.

season	AM	DY	EF	IF	SF	SM	UF
autumn	8	0	24	7	22	8	0
spring	16	7	31	19	29	18	29

Table 4. Pearson's Correlation Coefficient (r_p) matrix of environmental data (n = 437) used to assess drivers of hair cortisol for polar bears captured during spring in the Alaska Beaufort and Chukchi seas, 1983–1989 and 2004–2016. Correlated covariates indicated in bold font. Covariates: AO=annual Arctic Oscillation index for January–March, OW50=duration in days of sea ice <50% concentration over the Beaufort Sea continental shelf, OW15=duration in days of sea ice <15% concentration over the Beaufort Sea continental shelf, WS_MN=average annual wind speed in the Beaufort Sea during January–March, WS_SD=the standard deviation of wind speed.

	AO	OW50	OW15	WS_MN	WS_SD
AO	1	0.15	0.36	-0.34	-0.31
OW50		1	**0.76**	-0.58	-0.51
OW15			1	-0.35	-0.32
WS_MN				1	**0.90**
WS_SD					1

Table 5. The top model using environmental covariates to explain hair cortisol concentration in hair of polar bears captured during spring in the Alaska Beaufort, Bering and Chukchi seas, 1983–1989 and 2004–2016. See Table 4 for definitions of covariates, and Table S1 for parameter estimates of all 122 candidate models. Quadratics indicated by "^2", interactions indicated with "*".

terms	β	sd	t-value	*p*	df.residual	df.null	AIC	ΔAIC	AIC_w
Intercept	-9.0291	2.8925	-3.1215	0.0019					
AO	-19.8098	4.8371	-4.0954	0.0001					
AO*WS_SD	12.9044	2.9904	4.3153	0.0000					
OW15^2	-0.0024	0.0003	-7.8668	0.0000	431	436	2671.463	0.000	0.986
OW15	0.2419	0.0279	8.6695	0.0000					
WS_SD	8.1749	1.6882	4.8424	0.0000					

Table 6. Pearson's Correlation Coefficient (r_p) matrix of normalized morphometric data (n = 252) used to assess drivers of hair cortisol for polar bears captured during spring in the Alaska Beaufort, Bering and Chukchi seas, 1983–1989 and 2004–2016. Correlated covariates indicated in bold font. Covariates: SLBL=straight-line body length, HG=heart girth, M=body mass.

	SLBL	HG	M
SLBL	1	0.47	**0.61**
HG		1	**0.72**
M			1

Table 7. The top model using morphometric covariates (here, normalized body mass) to explain hair cortisol concentration in hair of polar bears captured during spring in the Alaska Beaufort, Bering and Chukchi seas, 1983–1989 and 2004–2016. M=mass. See Table S2 for parameter estimates on all 12 morphometric models. Quadratic indicated by "^2".

terms	β	sd	t-value	*p*	df.residual	df.null	AIC	ΔAIC	AIC_w
Intercept	8.1968	0.8552	9.5846	0.0000					
M^2	9.1507	3.6681	2.4947	0.0133	249	251	1403.507	0.000	0.486
M	-11.4758	3.7147	-3.0893	0.0022					

Figures

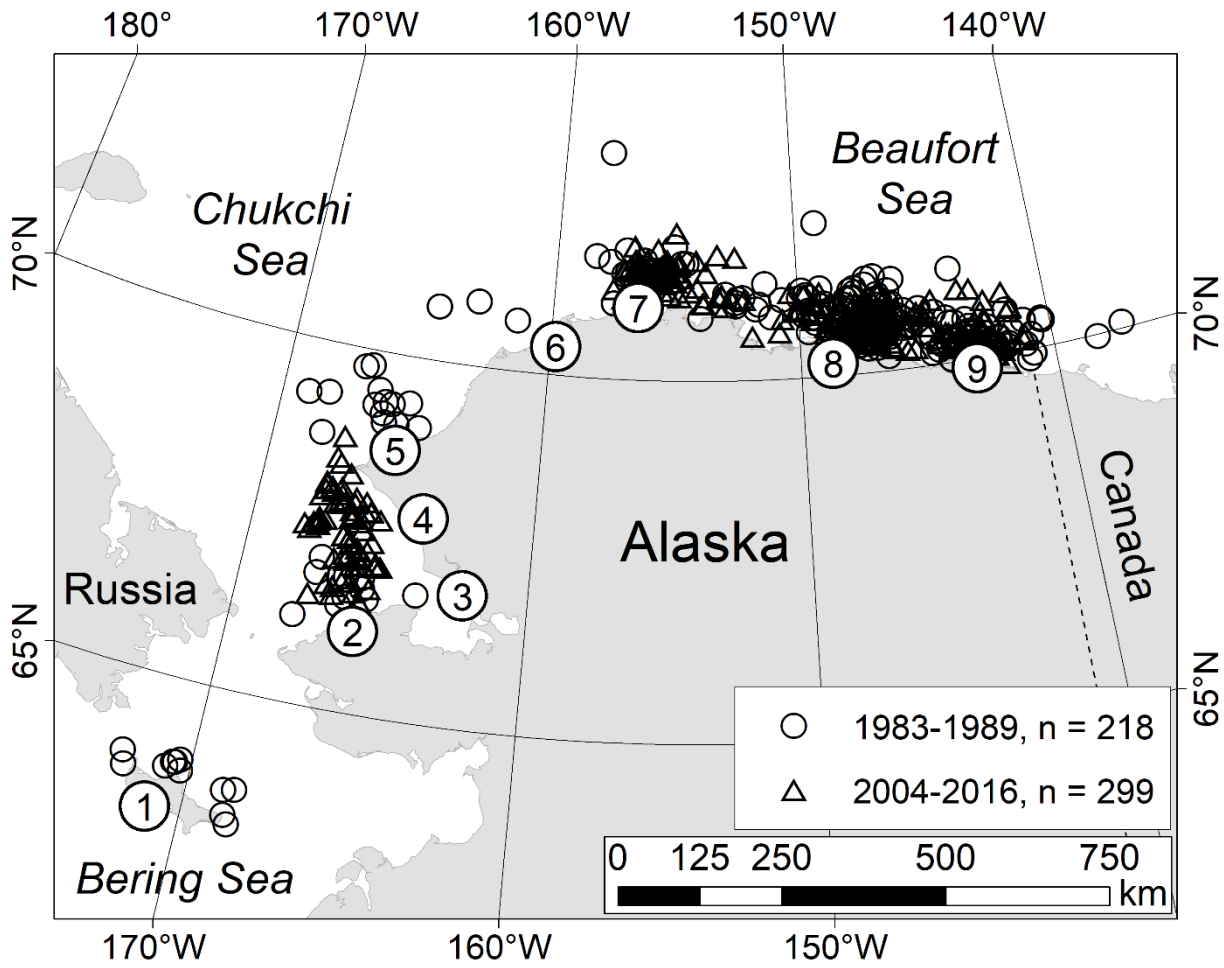

Figure 1. Distribution of hair samples assayed for cortisol and collected from polar bears captured in the Beaufort, Bering and Chukchi seas, 1983–1989 and 2004–2016 (n = 517). Place names mentioned in the text (numbers in circles): 1) St. Lawrence Island, 2) Shismaref, 3) Kotzebue, 4) Red Dog Mine port, 5) Cape Lisburne, 6) Wainwright, 7) Utqiagvik, 8) Deadhorse, and 9) Kaktovik.

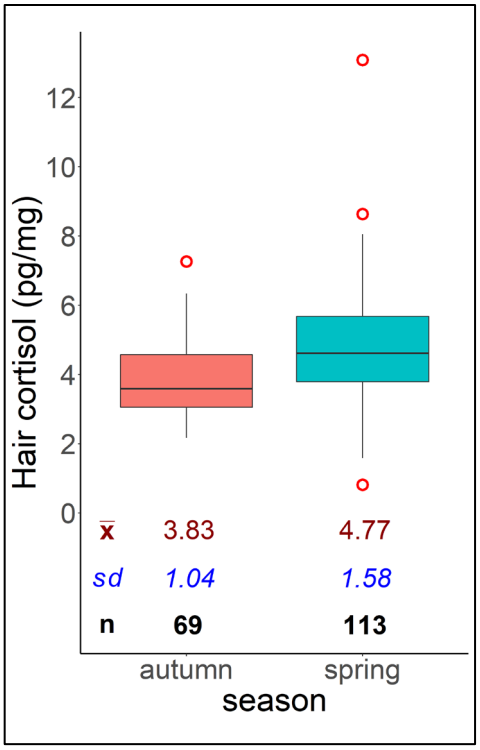

Figure 2. Box and whisker plots of hair cortisol concentration (HCC) for polar bears captured in the Beaufort, Bering and Chukchi seas during spring and autumn, 1983–1989. Spring HCC was significantly greater than HCC in autumn ($F_{1,170} = 22.564$, $p < 0.001$). Boxes represent the 25th and 75th quartiles and include the median. Whiskers are defined by the interquartile range (IQR; i.e., the maximum value minus the minimum value within the 75th and 25th quartiles), where lower whisker extent is the minimum data value in the 25th quartile - (1.5 × IQR), and upper whisker extent is the maximum data value in the 75th quartile + (1.5 × IQR). Outliers are represented by red circles beyond whiskers.

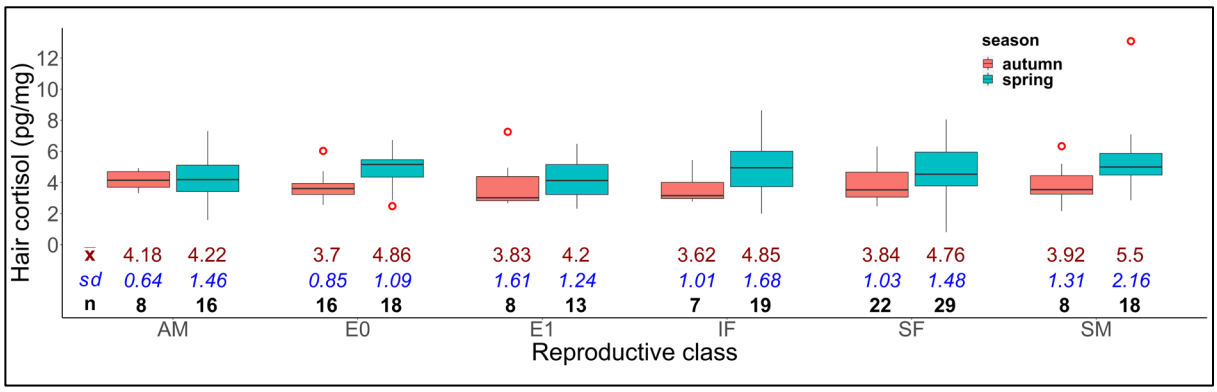

Figure 3. Box and whisker plots of hair cortisol concentration (HCC) for polar bears captured in the Beaufort, Bering and Chukchi seas during spring and autumn, 1983–1989, by reproductive class. HCC was not significantly different among reproductive status ($F_{1,170} = 1.285$, $p = 0.273$). AM = adult (≥ 5 years old) male, E0 = adult female encumbered by cubs-of-the-year (COY), E1 = adult female encumbered by yearling, IF = adult female independent of young, SF = subadult (2–4 years old) female, SM = subadult male. Boxes represent the 25th and 75th quartiles and include the median. Whiskers are defined by the interquartile range (IQR; i.e., the maximum value minus the minimum value within the 75th and 25th quartiles), where lower whisker extent is the minimum data value in the 25th quartile - (1.5 × IQR), and upper whisker extent is the maximum data value in the 75th quartile + (1.5 × IQR). Outliers are represented by red circles beyond whiskers.

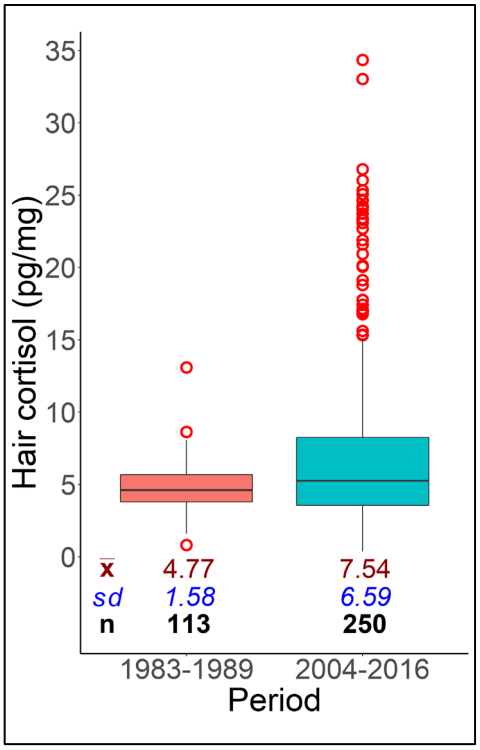

Figure 4. Box and whisker plots of hair cortisol concentration (HCC) for polar bears captured in the Alaska Beaufort, Bering and Chukchi seas in 1983–1989 and in 2004–2016. HCC in 2004–2016 was significantly greater than in 1983–1989 ($F_{1,351} = 9.004$, $p = 0.003$). Boxes represent the 25th and 75th quartiles and include the median. Whiskers are defined by the interquartile range (IQR; i.e., the maximum value minus the minimum value within the 75th and 25th quartiles), where lower whisker extent is the minimum data value in the 25th quartile - (1.5 × IQR), and upper whisker extent is the maximum data value in the 75th quartile + (1.5 × IQR). Outliers are represented by red circles beyond whiskers.

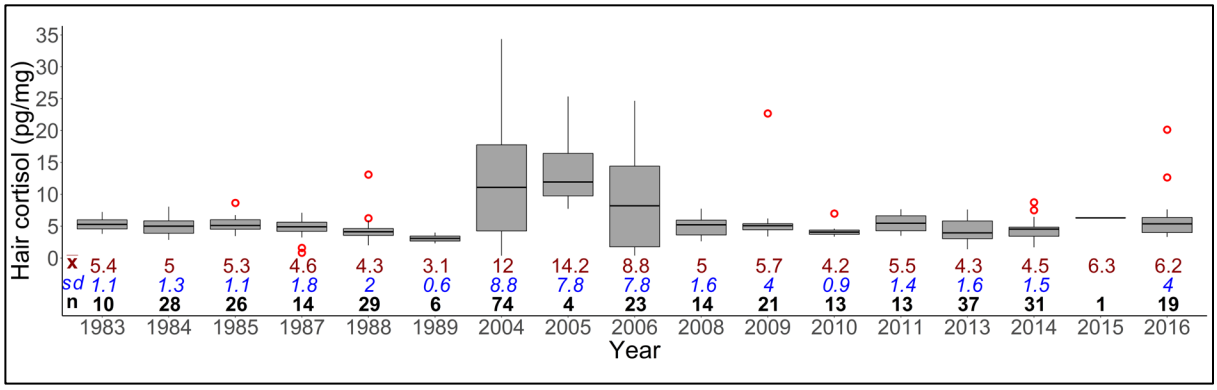

Figure 5. Box and whisker plots of hair cortisol concentration (HCC) for polar bears captured in the Alaska Beaufort, Bering and Chukchi seas during spring, 1983–2016. Greater HCC in 2004–2006 justified separating samples into three periods for subsequent analyses: 1983–1989, 2004–2006, and 2008–2016. No HCC samples were available for 1990–2003 nor for 2007. Boxes represent the 25th and 75th quartiles and include the median. Whiskers are defined by the interquartile range (IQR; i.e., the maximum value minus the minimum value within the 75th and 25th quartiles), where lower whisker extent is the minimum data value in the 25th quartile - (1.5 × IQR), and upper whisker extent is the maximum data value in the 75th quartile + (1.5 × IQR). Outliers are represented by red circles beyond whiskers.

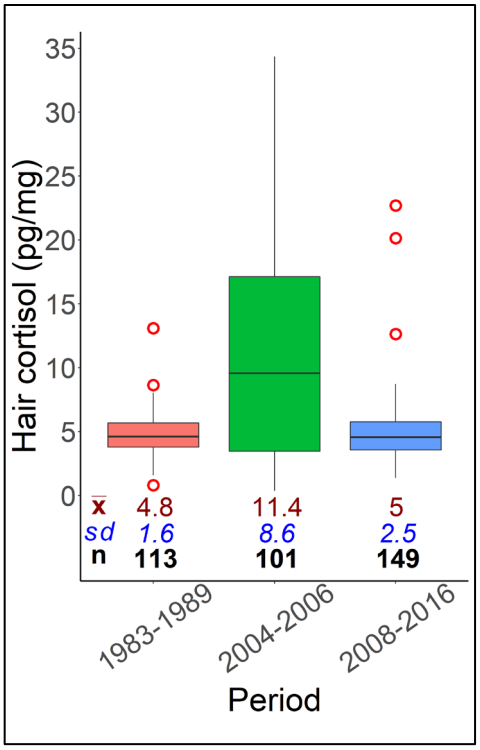

Figure 6. Box and whisker plots of hair cortisol concentration (HCC) for polar bears captured in the Alaska Beaufort, Bering and Chukchi seas during 1983–1989, 2004–2006, and 2008–2016. HCC during 2004–2006 was significantly greater than 1983–1989 and 2008–2016 ($F_{2,345} = 21.016$, $p < 0.001$). Boxes represent the 25th and 75th quartiles and include the median. Whiskers are defined by the interquartile range (IQR; i.e., the maximum value minus the minimum value within the 75th and 25th quartiles), where lower whisker extent is the minimum data value in the 25th quartile - (1.5 × IQR), and upper whisker extent is the maximum data value in the 75th quartile + (1.5 × IQR). Outliers are represented by red circles beyond whiskers.

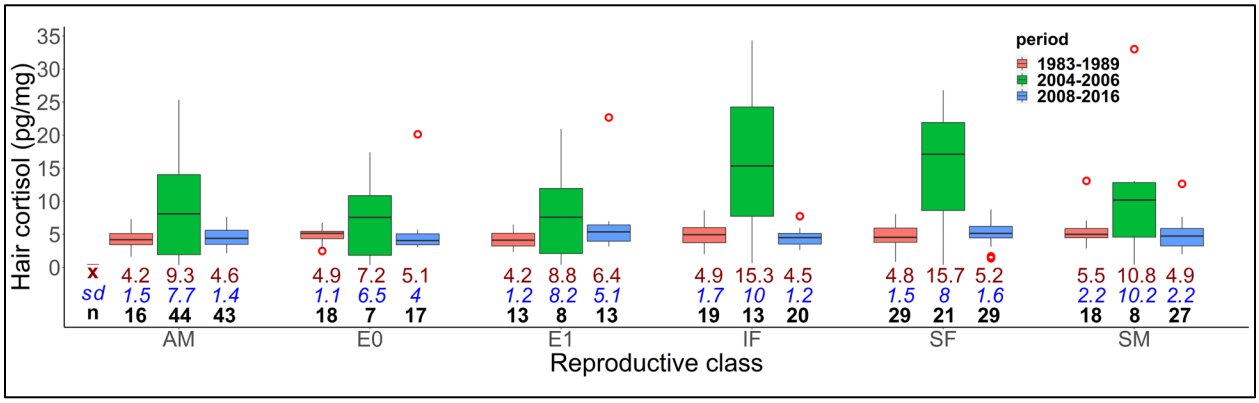

Figure 7. Box and whisker plots of hair cortisol concentration (HCC) for polar bears captured in the Alaska Beaufort, Bering and Chukchi seas during spring, for 1983–1989, 2004–2006, and 2008–2016, by period and reproductive class. HCC of IF and SF were significantly greater than several other reproductive classes ($F_{5,345} = 10.358$, $p < 0.001$) and there was an interaction between reproductive class and period ($F_{10,345} = 4.464$, $p < 0.001$; see text for details). Boxes represent the 25th and 75th quartiles and include the median. Whiskers are defined by the interquartile range (IQR; i.e., the maximum value minus the minimum value within the 75th and 25th quartiles), where lower whisker extent is the minimum data value in the 25th quartile - (1.5 × IQR), and upper whisker extent is the maximum data value in the 75th quartile + (1.5 × IQR). Outliers are represented by red circles beyond whiskers.

a)

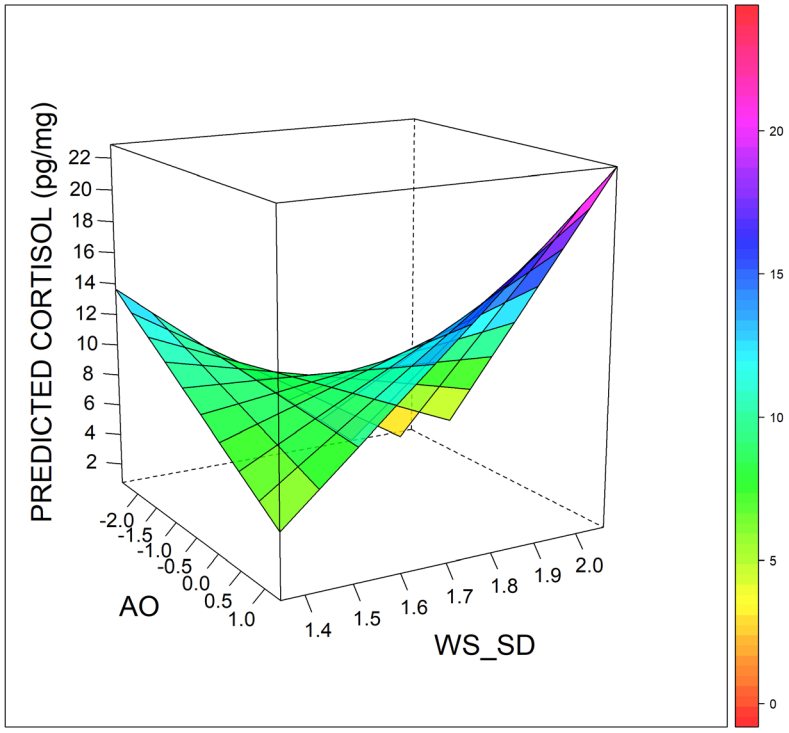

b)

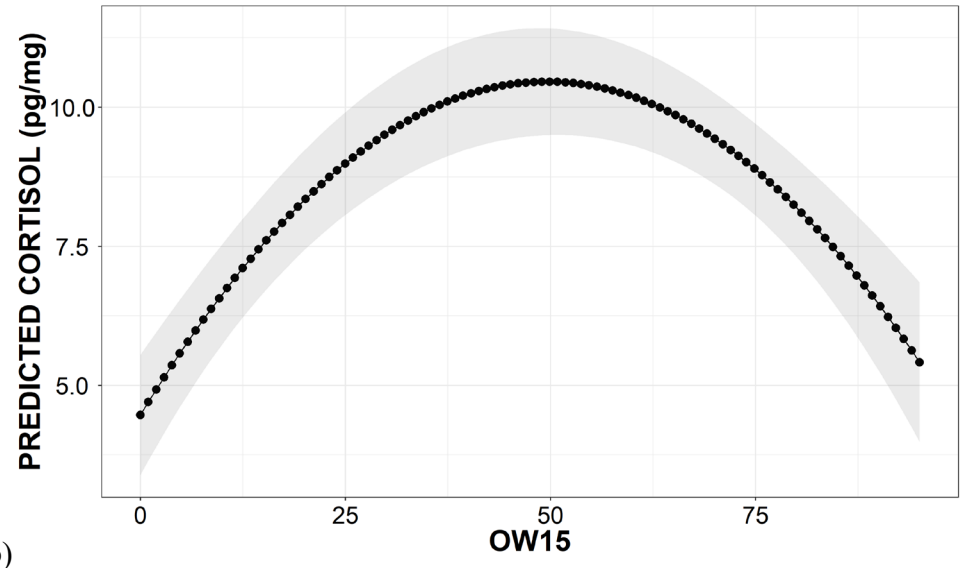

Figure 8. Predicted hair cortisol concentration (HCC) for polar bears, captured in the Alaska Beaufort, Bering and Chukchi seas during 1983–1989 and 2004–2016, in response to a) the Arctic Oscillation (AO) and the standard deviation of wind speed (WS_SD), and b) HCC (± 95% CI, shaded region) by duration of sea ice <15% concentration over the Beaufort Sea continental shelf. See Table 5 for the full model.

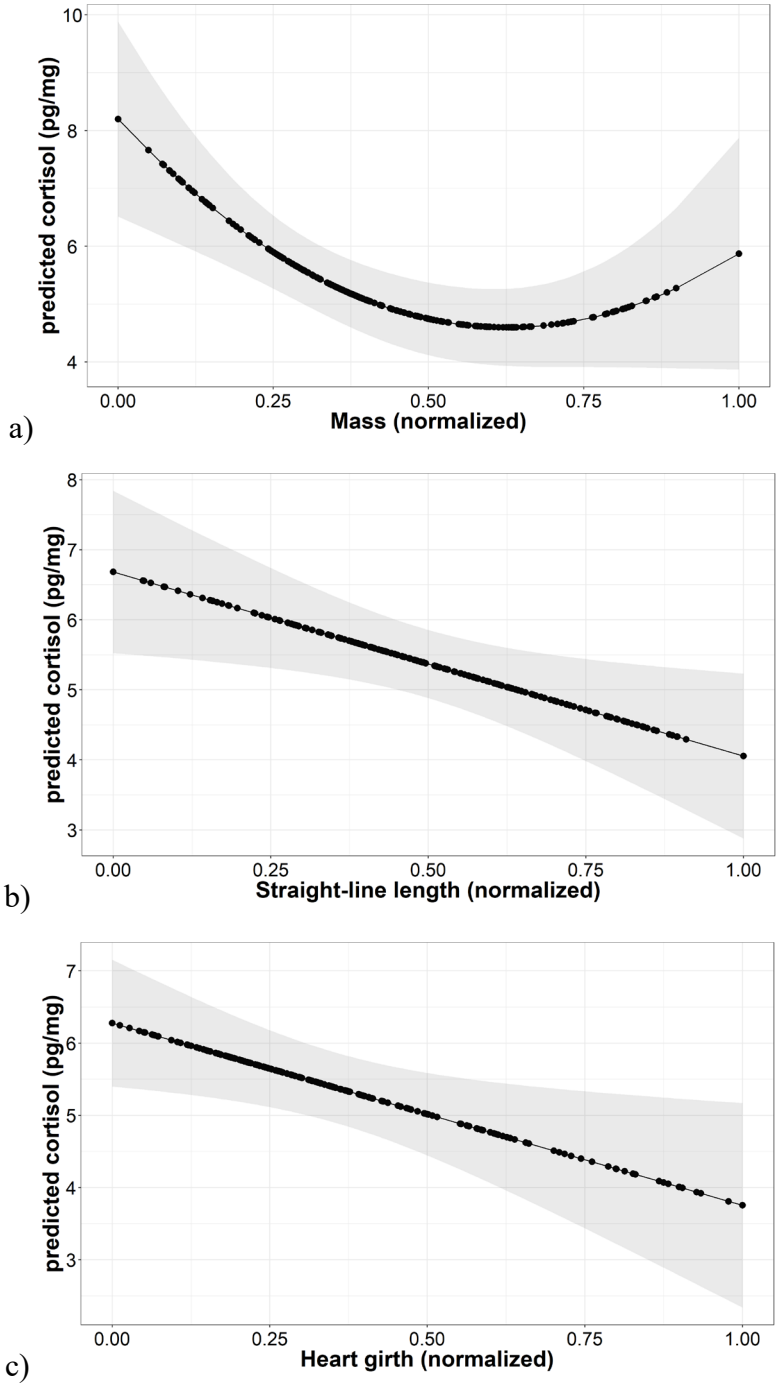

Figure 9. Predicted hair cortisol concentration (± 95% CI, shaded region) for polar bears, captured in the Alaska Beaufort, Bering and Chukchi seas during 1983–1989 and 2004–2016, in response to a) body mass, b) straight-line body length, and c) heart girth. All morphometrics were normalized by reproductive class.

Supplementary information

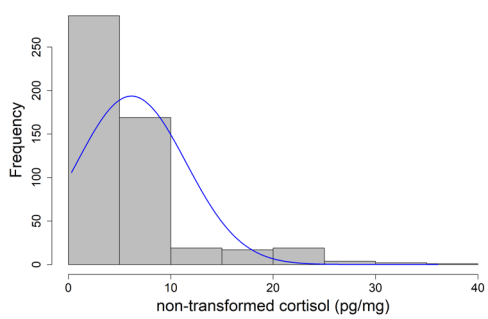

a)

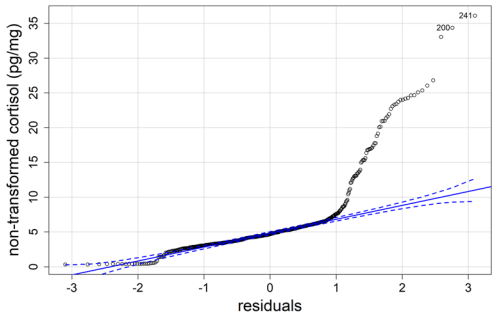

b)

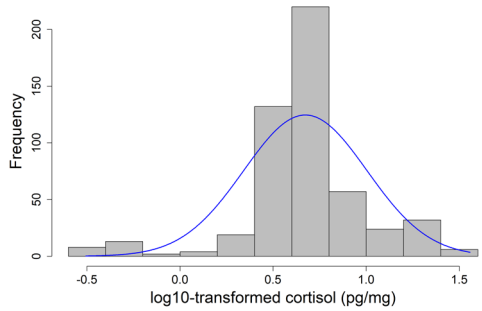

c)

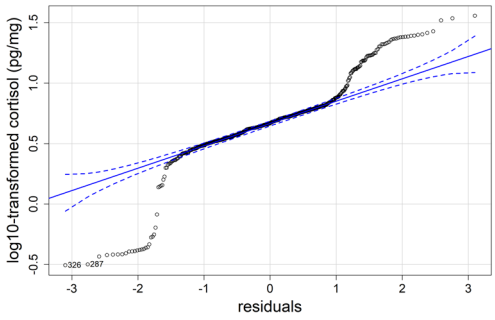

d)

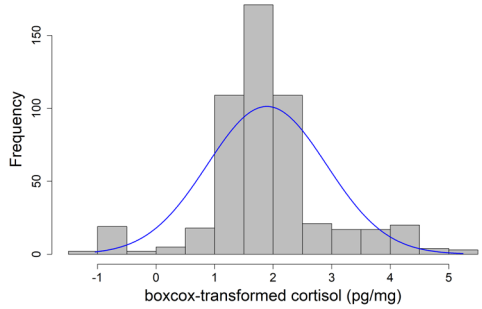

e)

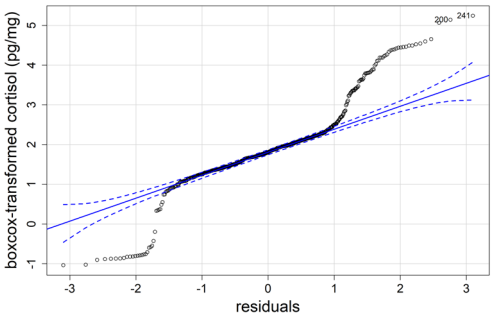

f)

Figure S1. Data distribution and qq plots of non-transformed (a, b), log transformed (c, d), and Box-Cox transformed (e, f) cortisol values. Not shown are square root transformed and inverse transform distributions. All transformations failed to achieve normality (all Shapiro-Wilks $p < 0.001$).

Table S1. Models (n = 122) using environmental covariates to explain hair cortisol concentration of polar bears captured during spring in the Alaska Beaufort, Bering and Chukchi seas, 1983–1989 and 2004–2016. See Table 4 for definitions of covariates. Quadratics indicated by "^2", interactions indicated with "*".

terms	β	SE	t	*p*	AIC	ΔAIC	AIC_w
Intercept	-9.029	2.893	-3.122	0.002	2671.46	0.00	0.99
AO	-19.810	4.837	-4.095	0.000			
AO*WS_SD	12.904	2.990	4.315	0.000			
OW15^2	-0.002	0.000	-7.867	0.000			
OW15	0.242	0.028	8.669	0.000			
WS_SD	8.175	1.688	4.842	0.000			
Intercept	5.460	3.610	1.512	0.131	2680.42	8.96	0.01
AO	1.610	0.365	4.411	0.000			
OW15*WS_SD	0.152	0.049	3.081	0.002			
OW15^2	-0.002	0.000	-4.795	0.000			
OW15	-0.085	0.101	-0.835	0.404			
WS_SD	0.051	2.054	0.025	0.980			
Intercept	-6.012	2.925	-2.056	0.040	2684.61	13.15	0.00
AO	-0.832	0.864	-0.963	0.336			
AO*OW15	0.029	0.013	2.301	0.022			
OW15^2	-0.003	0.000	-7.665	0.000			
OW15	0.270	0.036	7.437	0.000			
WS_SD	5.652	1.562	3.618	0.000			
Intercept	-31.602	4.319	-7.317	0.000	2686.66	15.19	0.00
AO	-9.104	4.258	-2.138	0.033			
AO*WS_SD	6.743	2.648	2.546	0.011			
OW50^2	-0.001	0.000	-3.692	0.000			
OW50	0.190	0.037	5.073	0.000			
WS_SD	17.140	1.957	8.760	0.000			
Intercept	-2.566	2.525	-1.016	0.310	2687.95	16.48	0.00
AO	1.022	0.314	3.253	0.001			
OW15^2	-0.002	0.000	-7.535	0.000			
OW15	0.216	0.028	7.771	0.000			
WS_SD	4.473	1.483	3.016	0.003			
Intercept	-7.336	5.012	-1.464	0.144	2688.94	17.48	0.00
AO	-22.753	7.846	-2.900	0.004			
AO*WS_MN	6.446	2.137	3.016	0.003			
OW15^2	-0.003	0.000	-8.247	0.000			
OW15	0.251	0.029	8.662	0.000			
WS_MN	3.161	1.321	2.393	0.017			

Continued next page

Table S1. Continued.

terms	β	SE	t	*p*	AIC	ΔAIC	AIC_w
Intercept	-27.742	4.419	-6.277	0.000	2689.12	17.66	0.00
AO	6.665	2.493	2.673	0.008			
AO*OW50	-0.038	0.019	-2.006	0.045			
OW50^2	-0.001	0.000	-3.849	0.000			
OW50	0.181	0.039	4.699	0.000			
WS_SD	15.588	1.886	8.263	0.000			
Intercept	3.490	7.274	0.480	0.632	2689.91	18.44	0.00
AO	0.870	0.493	1.765	0.078			
AO^2	-0.672	0.325	-2.069	0.039			
OW50*WS_SD	0.116	0.036	3.226	0.001			
OW50	-0.155	0.068	-2.291	0.022			
WS_SD	0.139	3.748	0.037	0.971			
Intercept	-15.084	3.298	-4.574	0.000	2690.44	18.98	0.00
AO	7.898	2.496	3.165	0.002			
AO*OW50	-0.061	0.019	-3.142	0.002			
AO^2	-1.164	0.317	-3.670	0.000			
OW50	0.045	0.010	4.460	0.000			
WS_SD	11.008	1.628	6.761	0.000			
Intercept	-29.939	4.297	-6.968	0.000	2691.18	19.72	0.00
AO	1.705	0.325	5.244	0.000			
OW50^2	-0.001	0.000	-4.105	0.000			
OW50	0.201	0.037	5.391	0.000			
WS_SD	15.754	1.891	8.330	0.000			
Intercept	-82.445	18.983	-4.343	0.000	2691.39	19.92	0.00
AO	9.542	2.570	3.713	0.000			
AO*OW50	-0.061	0.019	-3.160	0.002			
WS_SD^2	-24.738	6.995	-3.537	0.000			
OW50	0.016	0.012	1.342	0.180			
WS_SD	94.884	23.545	4.030	0.000			
Intercept	-13.399	15.097	-0.888	0.375	2691.86	20.40	0.00
AO	1.730	0.326	5.310	0.000			
OW50*WS_SD	0.066	0.058	1.143	0.254			
OW50^2	-0.001	0.000	-1.530	0.127			
OW50	0.024	0.160	0.148	0.883			
WS_SD	7.906	7.123	1.110	0.268			

Continued next page

Table S1. Continued.

terms	β	SE	t	*p*	AIC	ΔAIC	AIC_w
Intercept	6.993	7.101	0.985	0.325			
AO	1.646	0.322	5.118	0.000			
OW50*WS_SD	0.138	0.035	3.972	0.000	2692.23	20.76	0.00
OW50	-0.201	0.064	-3.131	0.002			
WS_SD	-1.426	3.685	-0.387	0.699			
Intercept	-12.557	28.684	-0.438	0.662			
AO	1.670	0.324	5.161	0.000			
OW50*WS_SD	0.120	0.043	2.762	0.006	2693.72	22.26	0.00
WS_SD^2	-6.019	8.557	-0.703	0.482			
OW50	-0.172	0.076	-2.251	0.025			
WS_SD	20.518	31.410	0.653	0.514			
Intercept	-4.135	5.072	-0.815	0.415			
AO	-0.596	0.901	-0.662	0.508			
AO*OW15	0.023	0.013	1.767	0.078	2694.91	23.45	0.00
OW15^2	-0.003	0.000	-7.739	0.000			
OW15	0.269	0.037	7.241	0.000			
WS_MN	2.101	1.269	1.655	0.099			
Intercept	4.869	0.548	8.888	0.000			
AO	0.821	0.310	2.650	0.008	2695.05	23.59	0.00
OW15^2	-0.003	0.000	-8.485	0.000			
OW15	0.231	0.028	8.340	0.000			
Intercept	-20.334	3.438	-5.915	0.000			
AO	-9.639	4.350	-2.216	0.027			
AO*WS_SD	6.307	2.779	2.270	0.024	2695.14	23.68	0.00
AO^2	-0.742	0.329	-2.254	0.025			
OW50	0.062	0.009	7.016	0.000			
WS_SD	12.852	1.823	7.050	0.000			
Intercept	4.149	0.826	5.021	0.000			
AO	-0.103	0.852	-0.121	0.904			
AO*OW15	0.014	0.012	1.164	0.245	2695.68	24.22	0.00
OW15^2	-0.003	0.000	-7.677	0.000			
OW15	0.259	0.037	7.047	0.000			
Intercept	8.677	6.913	1.255	0.210			
AO	1.166	0.368	3.171	0.002			
OW15*WS_MN	0.051	0.035	1.476	0.141	2695.86	24.40	0.00
OW15^2	-0.002	0.000	-6.668	0.000			
OW15	0.018	0.144	0.125	0.901			
WS_MN	-0.940	1.812	-0.519	0.604			

Continued next page

Table S1. Continued.

terms	β	SE	t	*p*	AIC	ΔAIC	AIC_w
Intercept	0.670	4.292	0.156	0.876			
AO	0.893	0.318	2.806	0.005			
OW15^2	-0.003	0.000	-7.963	0.000	2696.07	24.60	0.00
OW15	0.226	0.028	8.063	0.000			
WS_MN	1.132	1.147	0.987	0.324			
Intercept	-1.540	2.532	-0.608	0.543			
OW15^2	-0.002	0.000	-7.424	0.000	2696.52	25.06	0.00
OW15	0.223	0.028	7.953	0.000			
WS_SD	3.451	1.466	2.355	0.019			
Intercept	0.622	3.512	0.177	0.860			
OW15*WS_SD	0.038	0.043	0.888	0.375			
OW15^2	-0.002	0.000	-6.103	0.000	2697.72	26.26	0.00
OW15	0.148	0.088	1.680	0.094			
WS_SD	2.194	2.038	1.077	0.282			
Intercept	-53.215	21.623	-2.461	0.014			
AO	-7.774	5.092	-1.527	0.128			
AO*WS_SD	5.732	3.146	1.822	0.069	2698.04	26.58	0.00
WS_SD^2	-12.121	8.182	-1.481	0.139			
OW50	0.045	0.011	4.286	0.000			
WS_SD	53.918	27.079	1.991	0.047			
Intercept	-21.582	3.409	-6.331	0.000			
AO	-11.944	4.248	-2.811	0.005			
AO*WS_SD	8.241	2.655	3.104	0.002	2698.26	26.80	0.00
OW50	0.055	0.008	6.614	0.000			
WS_SD	13.888	1.772	7.836	0.000			
Intercept	-17.588	3.233	-5.440	0.000			
AO	0.184	0.450	0.410	0.682			
AO^2	-0.973	0.315	-3.092	0.002	2698.33	26.87	0.00
OW50	0.061	0.009	6.963	0.000			
WS_SD	11.031	1.645	6.707	0.000			
Intercept	-72.475	18.912	-3.832	0.000			
AO	1.483	0.319	4.650	0.000			
WS_SD^2	-20.145	6.913	-2.914	0.004	2699.39	27.93	0.00
OW50	0.037	0.010	3.870	0.000			
WS_SD	79.348	23.265	3.411	0.001			

Continued next page

Table S1. Continued.

terms	β	SE	t	*p*	AIC	ΔAIC	AIC_w
Intercept	11.497	3.603	3.191	0.002	2699.97	28.51	0.00
AO	1.409	0.525	2.684	0.008			
AO^2	-0.575	0.325	-1.770	0.077			
OW15*WS_SD	0.280	0.043	6.551	0.000			
OW15	-0.437	0.071	-6.186	0.000			
WS_SD	-2.864	2.090	-1.370	0.171			
Intercept	4.303	0.508	8.471	0.000	2700.08	28.62	0.00
OW15^2	-0.003	0.000	-8.272	0.000			
OW15	0.234	0.028	8.397	0.000			
Intercept	10.335	3.551	2.910	0.004	2701.14	29.67	0.00
AO	2.087	0.360	5.796	0.000			
OW15*WS_SD	0.279	0.043	6.500	0.000			
OW15	-0.441	0.071	-6.233	0.000			
WS_SD	-2.124	2.053	-1.034	0.301			
Intercept	-16.325	3.328	-4.906	0.000	2701.89	30.42	0.00
AO	7.345	2.527	2.907	0.004			
AO*OW50	-0.047	0.019	-2.447	0.015			
OW50	0.038	0.010	3.750	0.000			
WS_SD	11.811	1.637	7.217	0.000			
Intercept	2.838	4.255	0.667	0.505	2701.96	30.50	0.00
OW15^2	-0.003	0.000	-7.890	0.000			
OW15	0.232	0.028	8.239	0.000			
WS_MN	0.390	1.125	0.347	0.729			
Intercept	-16.563	28.641	-0.578	0.563	2702.23	30.77	0.00
AO	2.065	0.361	5.724	0.000			
OW15*WS_SD	0.235	0.063	3.703	0.000			
WS_SD^2	-8.525	9.008	-0.946	0.344			
OW15	-0.371	0.102	-3.639	0.000			
WS_SD	28.474	32.395	0.879	0.380			
Intercept	2.160	6.669	0.324	0.746	2703.94	32.48	0.00
OW15*WS_MN	-0.004	0.030	-0.132	0.895			
OW15^2	-0.003	0.000	-7.389	0.000			
OW15	0.248	0.125	1.981	0.048			
WS_MN	0.570	1.766	0.323	0.747			
Intercept	-18.176	3.259	-5.577	0.000	2705.90	34.44	0.00
AO	1.209	0.307	3.933	0.000			
OW50	0.052	0.008	6.215	0.000			
WS_SD	11.723	1.646	7.124	0.000			

Continued next page

Table S1. Continued.

terms	β	SE	t	*p*	AIC	ΔAIC	AIC_w
Intercept	-33.014	5.996	-5.506	0.000	2707.19	35.73	0.00
AO	-18.344	6.606	-2.777	0.006			
AO*WS_MN	5.008	1.814	2.761	0.006			
AO^2	-1.254	0.314	-3.987	0.000			
OW50	0.072	0.010	7.246	0.000			
WS_MN	8.960	1.464	6.120	0.000			
Intercept	-22.100	5.898	-3.747	0.000	2711.53	40.06	0.00
AO	4.520	2.610	1.732	0.084			
AO*OW50	-0.037	0.020	-1.816	0.070			
AO^2	-1.372	0.323	-4.254	0.000			
OW50	0.052	0.012	4.451	0.000			
WS_MN	6.589	1.366	4.822	0.000			
Intercept	-102.120	17.568	-5.813	0.000	2712.29	40.83	0.00
AO	1.653	0.321	5.152	0.000			
WS_SD^2	-33.932	6.019	-5.637	0.000			
WS_SD	122.932	20.683	5.944	0.000			
Intercept	-96.609	17.923	-5.390	0.000	2712.85	41.39	0.00
AO	2.818	0.787	3.582	0.000			
AO*OW15	-0.019	0.011	-1.741	0.082			
WS_SD^2	-32.738	6.176	-5.301	0.000			
OW15	-0.006	0.011	-0.570	0.569			
WS_SD	117.928	21.170	5.570	0.000			
Intercept	-26.089	5.488	-4.754	0.000	2712.85	41.39	0.00
AO	-0.147	0.449	-0.327	0.743			
AO^2	-1.255	0.317	-3.961	0.000			
OW50	0.064	0.010	6.691	0.000			
WS_MN	7.199	1.328	5.421	0.000			
Intercept	-100.289	17.840	-5.622	0.000	2713.92	42.45	0.00
AO	1.583	0.341	4.637	0.000			
WS_SD^2	-33.076	6.187	-5.346	0.000			
OW15	0.005	0.009	0.605	0.545			
WS_SD	120.216	21.179	5.676	0.000			
Intercept	-101.831	18.776	-5.424	0.000	2714.29	42.82	0.00
AO	1.447	4.707	0.307	0.759			
AO*WS_SD	0.128	2.919	0.044	0.965			
WS_SD^2	-33.819	6.556	-5.159	0.000			
WS_SD	122.572	22.269	5.504	0.000			

Continued next page

Table S1. Continued.

terms	β	SE	t	*p*	AIC	ΔAIC	AIC_w
Intercept	-19.299	13.842	-1.394	0.164	2714.57	43.10	0.00
AO	-0.071	0.471	-0.151	0.880			
AO^2	-1.227	0.321	-3.821	0.000			
OW50*WS_MN	0.014	0.027	0.534	0.593			
OW50	0.007	0.108	0.063	0.950			
WS_MN	5.502	3.441	1.599	0.111			
Intercept	-92.933	21.400	-4.343	0.000	2715.52	44.06	0.00
AO	-2.485	6.535	-0.380	0.704			
AO*WS_SD	2.487	3.990	0.623	0.533			
WS_SD^2	-30.057	7.862	-3.823	0.000			
OW15	0.010	0.012	0.867	0.386			
WS_SD	110.631	26.186	4.225	0.000			
Intercept	-0.851	7.133	-0.119	0.905	2715.95	44.49	0.00
OW50*WS_SD	0.077	0.034	2.296	0.022			
OW50	-0.090	0.062	-1.449	0.148			
WS_SD	2.212	3.719	0.595	0.552			
Intercept	-21.046	4.067	-5.175	0.000	2716.15	44.69	0.00
OW50^2	0.000	0.000	-2.252	0.025			
OW50	0.130	0.036	3.619	0.000			
WS_SD	11.648	1.773	6.568	0.000			
Intercept	-9.513	15.547	-0.612	0.541	2717.55	46.09	0.00
OW50*WS_SD	0.046	0.060	0.769	0.443			
OW50^2	0.000	0.000	-0.627	0.531			
OW50	0.006	0.165	0.036	0.972			
WS_SD	6.177	7.336	0.842	0.400			
Intercept	-5.191	29.486	-0.176	0.860	2717.93	46.46	0.00
OW50*WS_SD	0.073	0.044	1.670	0.096			
WS_SD^2	-1.329	8.757	-0.152	0.879			
OW50	-0.083	0.076	-1.088	0.277			
WS_SD	7.067	32.217	0.219	0.826			
Intercept	-43.848	18.303	-2.396	0.017	2718.74	47.28	0.00
WS_SD^2	-10.652	6.760	-1.576	0.116			
OW50	0.044	0.010	4.450	0.000			
WS_SD	45.466	22.614	2.010	0.045			
Intercept	-15.461	3.238	-4.775	0.000	2719.24	47.78	0.00
OW50	0.051	0.008	6.047	0.000			
WS_SD	9.922	1.607	6.175	0.000			

Continued next page

Table S1. Continued.

terms	β	SE	t	*p*	AIC	ΔAIC	AIC_w
Intercept	-32.140	6.094	-5.274	0.000			
AO	-17.104	6.711	-2.549	0.011			
AO*WS_MN	5.017	1.845	2.720	0.007	2721.02	49.56	0.00
OW50	0.057	0.009	6.109	0.000			
WS_MN	8.978	1.489	6.029	0.000			
Intercept	-95.705	58.624	-1.633	0.103			
AO	-11.695	8.345	-1.401	0.162			
AO*WS_MN	3.551	2.283	1.556	0.121	2721.82	50.36	0.00
WS_MN^2	-4.794	4.397	-1.090	0.276			
OW50	0.053	0.010	5.223	0.000			
WS_MN	44.077	32.230	1.368	0.172			
Intercept	-145.946	49.006	-2.978	0.003			
AO	1.276	0.322	3.967	0.000			
WS_MN^2	-8.825	3.559	-2.480	0.014	2722.27	50.80	0.00
OW50	0.046	0.009	5.059	0.000			
WS_MN	72.773	26.472	2.749	0.006			
Intercept	-31.827	6.189	-5.143	0.000			
AO	-18.001	7.349	-2.449	0.015			
AO*WS_MN	5.257	2.011	2.615	0.009	2722.93	51.47	0.00
OW50^2	0.000	0.000	0.301	0.763			
OW50	0.047	0.035	1.368	0.172			
WS_MN	8.976	1.491	6.021	0.000			
Intercept	-193.135	79.823	-2.420	0.016			
AO	1.226	0.329	3.729	0.000			
OW50*WS_MN	-0.028	0.037	-0.749	0.454	2723.70	52.23	0.00
WS_MN^2	-11.325	4.880	-2.321	0.021			
OW50	0.154	0.145	1.064	0.288			
WS_MN	94.601	39.375	2.403	0.017			
Intercept	-140.049	50.606	-2.767	0.006			
AO	2.538	2.684	0.946	0.345			
AO*OW50	-0.010	0.021	-0.474	0.636	2724.04	52.58	0.00
WS_MN^2	-8.472	3.639	-2.328	0.020			
OW50	0.042	0.012	3.651	0.000			
WS_MN	69.996	27.137	2.579	0.010			
Intercept	-25.201	5.575	-4.520	0.000			
AO	1.129	0.318	3.551	0.000	2726.44	54.98	0.00
OW50	0.050	0.009	5.506	0.000			
WS_MN	7.213	1.350	5.342	0.000			

Continued next page

Table S1. Continued.

terms	β	SE	t	*p*	AIC	ΔAIC	AIC_w
Intercept	-10.687	13.870	-0.770	0.441			
AO	1.232	0.330	3.729	0.000			
OW50*WS_MN	0.031	0.027	1.143	0.254	2727.12	55.66	0.00
OW50	-0.073	0.107	-0.677	0.498			
WS_MN	3.576	3.457	1.034	0.302			
Intercept	-23.039	6.009	-3.834	0.000			
AO	3.671	2.653	1.384	0.167			
AO*OW50	-0.020	0.020	-0.965	0.335	2727.50	56.04	0.00
OW50	0.042	0.012	3.626	0.000			
WS_MN	6.890	1.391	4.952	0.000			
Intercept	-26.770	5.918	-4.523	0.000			
AO	1.195	0.329	3.634	0.000			
OW50^2	0.000	0.000	-0.793	0.428	2727.81	56.34	0.00
OW50	0.075	0.033	2.259	0.024			
WS_MN	7.422	1.376	5.393	0.000			
Intercept	-11.938	3.064	-3.896	0.000			
AO	-18.188	5.162	-3.523	0.000			
AO*WS_SD	11.886	3.191	3.725	0.000	2728.10	56.63	0.00
OW15	0.035	0.010	3.514	0.000			
WS_SD	10.747	1.769	6.075	0.000			
Intercept	2.442	31.518	0.077	0.938			
AO	1.229	0.331	3.714	0.000			
OW50*WS_MN	0.055	0.058	0.944	0.346	2728.90	57.44	0.00
OW50^2	0.000	0.000	0.464	0.643			
OW50	-0.198	0.291	-0.681	0.496			
WS_MN	0.516	7.448	0.069	0.945			
Intercept	-11.023	3.185	-3.461	0.001			
AO	-17.818	5.173	-3.444	0.001			
AO*WS_SD	11.394	3.225	3.533	0.000	2728.98	57.51	0.00
AO^2	-0.357	0.339	-1.052	0.293			
OW15	0.038	0.010	3.667	0.000			
WS_SD	10.177	1.850	5.501	0.000			
Intercept	-24.568	6.471	-3.797	0.000			
AO	3.437	2.680	1.283	0.200			
AO*OW50	-0.018	0.021	-0.843	0.400	2729.09	57.62	0.00
OW50^2	0.000	0.000	-0.640	0.523			
OW50	0.064	0.036	1.795	0.073			
WS_MN	7.098	1.430	4.965	0.000			

Continued next page

Table S1. Continued.

terms	β	SE	t	*p*	AIC	ΔAIC	AIC_w
Intercept	22.318	7.182	3.108	0.002	2729.93	58.46	0.00
AO	0.581	0.522	1.111	0.267			
AO^2	-0.986	0.332	-2.969	0.003			
OW15*WS_MN	0.161	0.033	4.808	0.000			
OW15	-0.569	0.123	-4.615	0.000			
WS_MN	-4.191	1.897	-2.209	0.028			
Intercept	5.272	3.569	1.477	0.140	2731.87	60.40	0.00
OW15*WS_SD	0.163	0.039	4.147	0.000			
OW15	-0.240	0.064	-3.749	0.000			
WS_SD	0.113	2.091	0.054	0.957			
Intercept	-31.921	29.544	-1.080	0.281	2732.24	60.78	0.00
OW15*WS_SD	0.104	0.061	1.696	0.091			
WS_SD^2	-11.811	9.314	-1.268	0.205			
OW15	-0.146	0.098	-1.497	0.135			
WS_SD	42.473	33.469	1.269	0.205			
Intercept	5.736	1.240	4.624	0.000	2732.49	61.03	0.00
AO	7.111	2.619	2.715	0.007			
AO*OW50	-0.061	0.020	-3.020	0.003			
AO^2	-1.453	0.330	-4.398	0.000			
OW50	0.021	0.010	2.069	0.039			
Intercept	-72.693	17.211	-4.224	0.000	2733.14	61.68	0.00
WS_SD^2	-23.912	6.000	-3.985	0.000			
OW15	0.019	0.008	2.264	0.024			
WS_SD	87.486	20.435	4.281	0.000			
Intercept	-202.871	80.963	-2.506	0.013	2735.57	64.11	0.00
OW50*WS_MN	-0.056	0.037	-1.520	0.129			
WS_MN^2	-11.472	4.952	-2.317	0.021			
OW50	0.263	0.144	1.828	0.068			
WS_MN	97.496	39.951	2.440	0.015			
Intercept	-104.459	48.685	-2.146	0.032	2735.90	64.44	0.00
WS_MN^2	-6.226	3.557	-1.750	0.081			
OW50	0.045	0.009	4.854	0.000			
WS_MN	51.836	26.378	1.965	0.050			
Intercept	-75.172	17.258	-4.356	0.000	2736.28	64.82	0.00
WS_SD^2	-25.742	5.974	-4.309	0.000			
WS_SD	92.636	20.405	4.540	0.000			

Continued next page

Table S1. Continued.

terms	β	SE	t	*p*	AIC	ΔAIC	AIC_w
Intercept	18.060	7.101	2.543	0.011			
AO	1.662	0.378	4.402	0.000			
OW15*WS_MN	0.147	0.033	4.399	0.000	2736.77	65.31	0.00
OW15	-0.530	0.124	-4.285	0.000			
WS_MN	-3.022	1.872	-1.614	0.107			
Intercept	-19.766	5.432	-3.639	0.000			
OW50	0.048	0.009	5.221	0.000	2736.98	65.52	0.00
WS_MN	5.717	1.300	4.399	0.000			
Intercept	-5.822	2.555	-2.279	0.023			
AO	-8.492	4.419	-1.922	0.055	2738.41	66.95	0.00
AO*WS_SD	6.057	2.762	2.193	0.029			
WS_SD	7.975	1.604	4.972	0.000			
Intercept	-2.935	3.084	-0.951	0.342			
AO	2.360	0.806	2.927	0.004			
AO*OW15	-0.021	0.011	-1.852	0.065	2738.45	66.99	0.00
OW15	0.003	0.011	0.288	0.773			
WS_SD	6.032	1.663	3.628	0.000			
Intercept	-19.463	70.687	-0.275	0.783			
AO	1.625	0.384	4.230	0.000			
OW15*WS_MN	0.131	0.044	2.973	0.003	2738.48	67.02	0.00
WS_MN^2	-2.522	4.727	-0.534	0.594			
OW15	-0.473	0.164	-2.892	0.004			
WS_MN	16.481	36.601	0.450	0.653			
Intercept	-2.452	3.105	-0.790	0.430			
AO	1.681	0.964	1.744	0.082			
AO*OW15	-0.019	0.012	-1.621	0.106	2738.80	67.33	0.00
AO^2	-0.440	0.344	-1.280	0.201			
OW15	0.010	0.012	0.805	0.421			
WS_SD	5.648	1.688	3.345	0.001			
Intercept	-18.084	13.931	-1.298	0.195			
OW50*WS_MN	0.003	0.026	0.131	0.896	2738.97	67.50	0.00
OW50	0.034	0.105	0.322	0.748			
WS_MN	5.294	3.477	1.523	0.129			
Intercept	-19.570	5.655	-3.461	0.001			
OW50^2	0.000	0.000	0.127	0.899	2738.97	67.51	0.00
OW50	0.044	0.032	1.344	0.180			
WS_MN	5.698	1.310	4.349	0.000			

Continued next page

Table S1. Continued.

terms	β	SE	t	*p*	AIC	ΔAIC	AIC_w
Intercept	-4.921	2.711	-1.815	0.070			
AO	0.369	0.524	0.703	0.482			
AO^2	-0.530	0.340	-1.561	0.119	2739.45	67.99	0.00
OW15	0.022	0.010	2.309	0.021			
WS_SD	6.641	1.576	4.213	0.000			
Intercept	3.252	0.937	3.470	0.001			
AO	-0.681	0.452	-1.505	0.133	2739.62	68.16	0.00
AO^2	-1.259	0.327	-3.851	0.000			
OW50	0.037	0.008	4.377	0.000			
Intercept	-5.909	2.640	-2.238	0.026			
AO	1.000	0.334	2.997	0.003	2739.91	68.45	0.00
OW15	0.016	0.009	1.820	0.070			
WS_SD	7.274	1.526	4.768	0.000			
Intercept	-5.928	2.907	-2.039	0.042			
AO	-8.585	4.584	-1.873	0.062			
AO*WS_SD	6.131	2.929	2.093	0.037	2740.40	68.94	0.00
AO^2	0.025	0.327	0.077	0.939			
WS_SD	8.035	1.780	4.513	0.000			
Intercept	-2.611	31.952	-0.082	0.935			
OW50*WS_MN	0.032	0.059	0.539	0.590			
OW50^2	0.000	0.000	0.538	0.591	2740.67	69.21	0.00
OW50	-0.114	0.295	-0.388	0.698			
WS_MN	1.688	7.550	0.224	0.823			
Intercept	-3.966	2.421	-1.638	0.102			
AO	1.175	0.320	3.670	0.000	2741.24	69.78	0.00
WS_SD	6.617	1.486	4.452	0.000			
Intercept	-3.299	2.632	-1.254	0.211			
AO	0.962	0.459	2.096	0.037	2742.81	71.35	0.00
AO^2	-0.201	0.310	-0.649	0.517			
WS_SD	6.278	1.576	3.983	0.000			
Intercept	-145.735	51.372	-2.837	0.005			
AO	2.581	0.836	3.088	0.002			
AO*OW15	-0.024	0.012	-1.952	0.052	2743.51	72.04	0.00
WS_MN^2	-10.473	3.650	-2.869	0.004			
OW15	-0.002	0.012	-0.200	0.842			
WS_MN	80.306	27.391	2.932	0.004			

Continued next page

Table S1. Continued.

terms	β	SE	t	*p*	AIC	ΔAIC	AIC_w
Intercept	-12.650	5.298	-2.388	0.017	2745.27	73.80	0.00
AO	-23.421	8.590	-2.726	0.007			
AO*WS_MN	6.324	2.316	2.730	0.007			
AO^2	-0.944	0.341	-2.768	0.006			
OW15	0.043	0.012	3.487	0.001			
WS_MN	4.949	1.387	3.567	0.000			
Intercept	-168.891	50.147	-3.368	0.001	2745.35	73.89	0.00
AO	1.092	0.343	3.185	0.002			
WS_MN^2	-11.722	3.605	-3.252	0.001			
OW15	0.013	0.009	1.429	0.154			
WS_MN	90.929	26.933	3.376	0.001			
Intercept	-167.191	50.193	-3.331	0.001	2745.42	73.95	0.00
AO	1.225	0.331	3.705	0.000			
WS_MN^2	-11.767	3.609	-3.260	0.001			
WS_MN	90.818	26.965	3.368	0.001			
Intercept	-191.487	57.351	-3.339	0.001	2746.64	75.18	0.00
AO	7.943	7.673	1.035	0.301			
AO*WS_MN	-1.838	2.097	-0.876	0.381			
WS_MN^2	-13.617	4.182	-3.256	0.001			
WS_MN	104.220	31.005	3.361	0.001			
Intercept	-4.893	2.643	-1.851	0.065	2746.88	75.42	0.00
OW15	0.023	0.008	2.779	0.006			
WS_SD	6.263	1.502	4.171	0.000			
Intercept	-161.629	63.003	-2.565	0.011	2747.32	75.85	0.00
AO	-0.997	10.956	-0.091	0.928			
AO*WS_MN	0.567	2.970	0.191	0.849			
WS_MN^2	-11.146	4.706	-2.368	0.018			
OW15	0.014	0.012	1.143	0.254			
WS_MN	86.812	34.535	2.514	0.012			
Intercept	7.657	0.720	10.640	0.000	2748.00	76.53	0.00
AO	2.118	0.966	2.192	0.029			
AO*OW15	-0.033	0.011	-3.006	0.003			
AO^2	-0.645	0.342	-1.884	0.060			
OW15	-0.002	0.012	-0.199	0.843			

Continued next page

Table S1. Continued.

terms	β	SE	t	*p*	AIC	ΔAIC	AIC_w
Intercept	1.043	5.348	0.195	0.846	2748.42	76.96	0.00
AO	1.773	1.005	1.765	0.078			
AO*OW15	-0.026	0.012	-2.074	0.039			
AO^2	-0.624	0.342	-1.823	0.069			
OW15	0.004	0.013	0.345	0.730			
WS_MN	1.685	1.350	1.248	0.213			
Intercept	7.970	0.702	11.347	0.000	2749.57	78.11	0.00
AO	3.190	0.784	4.070	0.000			
AO*OW15	-0.038	0.011	-3.573	0.000			
OW15	-0.014	0.010	-1.341	0.181			
Intercept	6.089	1.264	4.818	0.000	2749.63	78.17	0.00
AO	6.335	2.667	2.375	0.018			
AO*OW50	-0.044	0.020	-2.165	0.031			
OW50	0.009	0.010	0.904	0.367			
Intercept	0.885	5.362	0.165	0.869	2749.78	78.31	0.00
AO	2.785	0.840	3.316	0.001			
AO*OW15	-0.030	0.012	-2.473	0.014			
OW15	-0.006	0.012	-0.510	0.610			
WS_MN	1.802	1.352	1.333	0.183			
Intercept	-4.951	4.518	-1.096	0.274	2750.76	79.30	0.00
AO	-0.011	0.520	-0.022	0.982			
AO^2	-0.764	0.337	-2.266	0.024			
OW15	0.022	0.010	2.271	0.024			
WS_MN	2.996	1.198	2.502	0.013			
Intercept	-12.940	5.337	-2.425	0.016	2750.97	79.50	0.00
AO	-17.759	8.407	-2.112	0.035			
AO*WS_MN	5.082	2.290	2.219	0.027			
OW15	0.028	0.011	2.498	0.013			
WS_MN	5.085	1.397	3.639	0.000			
Intercept	6.586	1.621	4.063	0.000	2751.39	79.93	0.00
AO	6.452	2.681	2.407	0.017			
AO*OW50	-0.045	0.021	-2.205	0.028			
OW50^2	0.000	0.000	0.491	0.624			
OW50	-0.007	0.033	-0.205	0.837			
Intercept	4.201	0.919	4.573	0.000	2752.34	80.87	0.00
AO	0.599	0.312	1.923	0.055			
OW50	0.022	0.008	2.905	0.004			

Continued next page

Table S1. Continued.

terms	β	SE	t	*p*	AIC	ΔAIC	AIC_w
Intercept	-1.476	2.357	-0.626	0.531	2752.59	81.13	0.00
WS_SD	4.920	1.433	3.434	0.001			
Intercept	-136.555	49.624	-2.752	0.006	2753.50	82.03	0.00
WS_MN^2	-9.574	3.578	-2.676	0.008			
OW15	0.020	0.009	2.354	0.019			
WS_MN	74.015	26.681	2.774	0.006			
Intercept	-6.465	4.489	-1.440	0.151	2753.92	82.46	0.00
AO	0.884	0.341	2.594	0.010			
OW15	0.013	0.009	1.442	0.150			
WS_MN	3.432	1.188	2.890	0.004			
Intercept	-2.228	4.377	-0.509	0.611	2753.95	82.48	0.00
AO	0.559	0.458	1.220	0.223			
AO^2	-0.440	0.307	-1.433	0.153			
WS_MN	2.535	1.186	2.138	0.033			
Intercept	9.714	6.987	1.390	0.165	2753.95	82.49	0.00
OW15*WS_MN	0.078	0.030	2.589	0.010			
OW15	-0.266	0.110	-2.409	0.016			
WS_MN	-1.075	1.858	-0.579	0.563			
Intercept	-4.096	4.183	-0.979	0.328	2754.01	82.55	0.00
AO	1.018	0.328	3.104	0.002			
WS_MN	2.978	1.146	2.597	0.010			
Intercept	3.812	0.899	4.241	0.000	2754.04	82.58	0.00
OW50	0.024	0.008	3.211	0.001			
Intercept	-81.083	70.509	-1.150	0.251	2754.26	82.80	0.00
OW15*WS_MN	0.044	0.040	1.107	0.269			
WS_MN^2	-6.133	4.739	-1.294	0.196			
OW15	-0.142	0.146	-0.968	0.334			
WS_MN	46.246	36.614	1.263	0.207			
Intercept	4.420	1.295	3.413	0.001	2754.28	82.82	0.00
AO	0.584	0.319	1.833	0.068			
OW50^2	0.000	0.000	0.240	0.810			
OW50	0.015	0.032	0.456	0.649			
Intercept	6.266	0.556	11.266	0.000	2755.04	83.58	0.00
AO	-0.370	0.503	-0.736	0.462			
AO^2	-0.899	0.335	-2.687	0.007			
OW15	0.018	0.010	1.863	0.063			

Continued next page

Table S1. Continued.

terms	β	SE	t	*p*	AIC	ΔAIC	AIC_w
Intercept	-5.268	4.391	-1.200	0.231			
AO	-4.833	6.667	-0.725	0.469	2755.24	83.77	0.00
AO*WS_MN	1.609	1.831	0.879	0.380			
WS_MN	3.332	1.216	2.741	0.006			
Intercept	-3.299	4.628	-0.713	0.476			
AO	-4.212	6.677	-0.631	0.529			
AO*WS_MN	1.319	1.842	0.716	0.474	2755.43	83.97	0.00
AO^2	-0.414	0.309	-1.338	0.182			
WS_MN	2.852	1.266	2.252	0.025			
Intercept	4.394	1.298	3.384	0.001			
OW50^2	0.000	0.000	0.622	0.535	2755.66	84.19	0.00
OW50	0.005	0.032	0.160	0.873			
Intercept	7.102	0.330	21.527	0.000			
AO	0.154	0.419	0.367	0.714	2756.53	85.07	0.00
AO^2	-0.611	0.298	-2.052	0.041			
Intercept	-126.831	49.710	-2.551	0.011			
WS_MN^2	-9.201	3.594	-2.560	0.011	2757.06	85.59	0.00
WS_MN	70.275	26.773	2.625	0.009			
Intercept	-4.311	4.441	-0.971	0.332			
OW15	0.019	0.009	2.222	0.027	2758.66	87.20	0.00
WS_MN	2.695	1.161	2.322	0.021			
Intercept	6.744	0.281	24.000	0.000	2758.75	87.29	0.00
AO	0.732	0.311	2.353	0.019			
Intercept	6.409	0.558	11.495	0.000			
AO	0.648	0.333	1.944	0.053	2760.27	88.81	0.00
OW15	0.006	0.009	0.694	0.488			
Intercept	0.038	4.004	0.010	0.992	2761.61	90.14	0.00
WS_MN	1.782	1.090	1.634	0.103			
Intercept	5.935	0.503	11.799	0.000	2762.06	90.60	0.00
OW15	0.012	0.008	1.489	0.137			

Table S2. Models (n = 12) using environmental covariates to explain hair cortisol concentration of polar bears captured during spring in the Alaska Beaufort, Bering and Chukchi seas, 1983–1989 and 2004–2016. Quadratics indicated by "^2", interactions indicated with "*".

terms	β	SE	t	*p*	AIC	ΔAIC	AIC_w
Intercept	8.197	0.855	9.585	0.000			
M^2	9.151	3.668	2.495	0.013	1403.51	0.00	0.49
M	-11.476	3.715	-3.089	0.002			
Intercept	7.886	0.925	8.525	0.000			
HG	-4.976	2.577	-1.931	0.055	1407.34	3.83	0.07
SLBL*HG	6.144	4.301	1.428	0.154			
SLBL	-3.983	1.948	-2.045	0.042			
Intercept	6.882	0.603	11.418	0.000			
HG	-1.703	1.181	-1.443	0.150	1407.40	3.89	0.07
SLBL	-1.808	1.217	-1.485	0.139			
Intercept	6.684	0.588	11.364	0.000	1407.50	3.99	0.07
SLBL	-2.629	1.078	-2.438	0.015			
Intercept	6.277	0.446	14.085	0.000	1407.62	4.12	0.06
HG	-2.523	1.046	-2.412	0.017			
Intercept	6.534	0.542	12.066	0.000	1407.73	4.22	0.06
M	-2.610	1.092	-2.390	0.018			
Intercept	7.560	0.955	7.914	0.000			
HG	-1.744	1.182	-1.476	0.141	1408.55	5.05	0.04
SLBL^2	3.360	3.673	0.915	0.361			
SLBL	-5.166	3.868	-1.336	0.183			
Intercept	7.316	0.943	7.757	0.000			
SLBL^2	3.154	3.679	0.857	0.392	1408.76	5.25	0.04
SLBL	-5.800	3.853	-1.505	0.134			
Intercept	6.662	0.695	9.588	0.000			
HG	-4.887	3.437	-1.422	0.156	1409.10	5.59	0.03
HG^2	2.499	3.462	0.722	0.471			
Intercept	8.082	1.056	7.657	0.000			
HG	-4.616	2.742	-1.683	0.094			
SLBL*HG	5.432	4.681	1.161	0.247	1409.18	5.67	0.03
SLBL^2	1.552	3.987	0.389	0.698			
SLBL	-5.282	3.867	-1.366	0.173			

Continued next page

Table S2. Continued.

terms	β	SE	t	*p*	AIC	ΔAIC	AIC_w
Intercept	7.029	0.746	9.422	0.000	1409.29	5.78	0.03
HG	-2.895	3.741	-0.774	0.440			
HG^2	1.206	3.589	0.336	0.737			
SLBL	-1.693	1.266	-1.337	0.182			
Intercept	7.856	0.953	8.245	0.000	1409.32	5.81	0.03
HG	-4.586	3.926	-1.168	0.244			
HG^2	-0.500	3.786	-0.132	0.895			
SLBL*HG	6.339	4.555	1.392	0.165			
SLBL	-4.100	2.142	-1.914	0.057			